

1 **Microfluidic antibody profiling after repeated SARS-CoV-2 vaccination links antibody**
2 **affinity and concentration to impaired immunity and variant escape in patients on anti-**
3 **CD-20 therapy**

4

5 **Authors**

6 Ashley Priddey¹, Michael Xin Hua Chen-Xu², Daniel James Cooper², Serena MacMillan¹,
7 Georg Meisl³, Catherine K Xu³, Myra Hosmillo⁴, Ian G. Goodfellow⁴, Rafael Kollyfas⁵,
8 Rainer Doffinger⁶, John R Bradley², Irina I Mohorianu⁵, Rachel Jones², Tuomas P.J.
9 Knowles^{3, 7}, Rona Smith², V Kosmoliaptsis^{1, 8 *}

10

11 **Affiliations**

12 ¹Department of Surgery, University of Cambridge, Addenbrooke's Hospital, Hills Road,
13 Cambridge CB2 0QQ, UK

14 ²Department of Medicine, University of Cambridge School of Clinical Medicine, Cambridge,
15 UK and Cambridge University Hospitals NHS Foundation Trust, Cambridge, UK

16 ³Centre for Misfolding Diseases, Yusuf Hamied Department of Chemistry, University of
17 Cambridge, Lensfield Road, Cambridge CB2 1EW, UK

18 ⁴Department of Pathology, Division of Virology, University of Cambridge, Cambridge, UK

19 ⁵Wellcome-MRC Cambridge Stem Cell Institute, Jeffrey Cheah Biomedical Centre,
20 University of Cambridge, CB2 0AW, UK

21 ⁶Department of Clinical Biochemistry and Immunology, Addenbrooke's Hospital, Cambridge
22 CB2 0QQ, UK

23 ⁷Cavendish Laboratory, Department of Physics, University of Cambridge, JJ Thomson Ave,
24 Cambridge CB3 0HE, UK

1 ⁸NIHR Blood and Transplant Research Unit in Organ Donation and Transplantation at the
2 University of Cambridge and the NIHR Cambridge Biomedical Research Centre, Cambridge,
3 UK

4 **Running title: Anti-SARS-CoV-2 antibody affinity profiling in Rituximab-treated**
5 **patients**

6 Number of words: 4,983

7 Number of figures: 8

8 Number of Tables: 0

9 *** Corresponding author:**

10 Dr Vasilis Kosmoliaptis

11 vk256@cam.ac.uk

12 **Key words:**

13 Antibody affinity, Rituximab, SARS-CoV-2 vaccination, neutralisation capacity, Omicron
14 (B.1.1.529), antibody concentration, immunocompromised, SARS-CoV-2 infection

15

1 **Abstract**

2 **Background:** Patients with autoimmune/inflammatory conditions on anti-CD20 therapies,
3 such as Rituximab, have suboptimal humoral responses to vaccination and are vulnerable to
4 poorer clinical outcomes following SARS-CoV-2 infection. We aimed to examine how the
5 fundamental parameters of antibody responses, namely affinity and concentration, shape the
6 quality of humoral immunity after vaccination in these patients.

7 **Methods:** We performed in depth antibody characterisation in sera collected four to six
8 weeks after each of three vaccine doses to wild-type (WT) SARS-CoV-2 in Rituximab-
9 treated primary vasculitis patients (n=14) using Luminex and pseudovirus neutralisation
10 assays, whereas a novel microfluidic-based immunoassay was used to quantify polyclonal
11 antibody affinity and concentration against both WT and Omicron (B.1.1.529) variants.
12 Comparative antibody profiling was performed at equivalent time points in healthy
13 individuals after three antigenic exposures to WT SARS-CoV-2 (one infection and two
14 vaccinations; n=15) and in convalescent patients after WT SARS-CoV-2 infection (n=30).

15 **Results:** Rituximab-treated patients had lower antibody levels and neutralisation titres against
16 both WT and Omicron SARS-CoV-2 variants compared to healthy individuals. Neutralisation
17 capacity was weaker against Omicron versus WT both in Rituximab-treated patients and in
18 healthy individuals. In the Rituximab cohort, this was driven by lower antibody affinity
19 against Omicron versus WT (median [range] K_D : 21.6 [9.7-38.8] nM vs 4.6 [2.3-44.8] nM,
20 $p=0.0004$). By contrast, healthy individuals with hybrid immunity produced a broader
21 antibody response, a subset of which recognised Omicron with higher affinity than antibodies
22 in Rituximab-treated patients (median [range] K_D : 1.05 [0.45-1.84] nM vs 20.25 [13.2-38.8]
23 nM, $p=0.0002$), underpinning the stronger serum neutralisation capacity against Omicron in
24 the former group. Rituximab-treated patients had similar anti-WT antibody levels and
25 neutralisation titres to unvaccinated convalescent individuals, despite two more exposures to

1 SARS-CoV-2 antigen. Temporal profiling of the antibody response showed evidence of
2 affinity maturation in healthy convalescent patients after a single SARS-CoV-2 infection
3 which was not observed in Rituximab-treated patients, despite repeated vaccination.
4 **Discussion:** Our results enrich previous observations of impaired humoral immune responses
5 to SARS-CoV-2 in Rituximab-treated patients and highlight the significance of quantitative
6 assessment of serum antibody affinity and concentration in monitoring anti-viral immunity,
7 viral escape, and the evolution of the humoral response.

8

1 **Introduction**

2 SARS-CoV-2 infection (COVID-19) is of ongoing clinical concern for patients with primary
3 systemic vasculitis, particularly those receiving repeated dosing with B cell depleting
4 therapies, such as the anti-CD20 agent, Rituximab. Patients with autoimmune/inflammatory
5 conditions on immunosuppressive therapy, particularly those on anti-CD20 therapies(1, 2),
6 are vulnerable to poorer clinical outcomes following SARS-CoV-2 infection, including
7 hospitalisation and death(3, 4). Given this, and the suboptimal humoral immune responses
8 after SARS-CoV-2 vaccination observed in those receiving anti-CD20 therapies(5-7),
9 subsequent SARS-CoV-2 vaccine doses i.e., “boosters”, have been recommended for these
10 patient groups in several jurisdictions(8-10), including those with primary systemic
11 vasculitis(11).

12 Humoral immune responses after primary vaccination using vaccines targeted against the
13 original (ancestral, wild-type) strain of SARS-CoV-2 e.g., the mRNA vaccines Pfizer
14 BioNTech BNT162b2 (Pfizer) and mRNA-1273 (Moderna) or the adenovirus-vector based
15 vaccines Oxford-AstraZeneca ChAdOx1 nCoV-19 (AZ) or Ad26.COV2-S
16 (Johnson&Johnson), are often suboptimal among patients receiving anti-CD20 therapies.
17 Specifically, titres of antibodies directed against the spike protein subunit (anti-spike IgG)
18 and/or receptor binding domain (anti-RBD IgG) of SARS-CoV-2 and the proportion of
19 patients on anti-CD20 therapy who seroconvert following primary vaccination are lower
20 compared to those not on such therapy and healthy controls(5, 6, 12, 13). Furthermore, of
21 patients on anti-CD20 therapies who seroconvert after primary vaccination, many have lower
22 neutralisation titres compared to those on other immunosuppressants and healthy controls(14-
23 16). Although neutralising antibody titres and, to a lesser extent, anti-spike IgG and anti-RBD
24 IgG titres, derived from primary vaccination with vaccines targeting the original strain of
25 SARS-CoV-2 correlate with protection against symptomatic infection from the ancestral

1 virus(17), significant reductions in the neutralisation capacity of these antibodies have been
2 observed against subsequent SARS-CoV-2 variants of concern, such the B.1.617.2 variant
3 (Delta)(17) and the B.1.1.529 variant and its sublineages (Omicron)(18-20), which harbour
4 mutations in the spike protein that modify the critical domain for virus-neutralising
5 antibodies(21, 22). SARS-CoV-2 specific T cell responses following vaccination, which may
6 be protective against severe infection(23, 24), appear largely preserved among anti-CD20
7 treated patients(5) although the clinical significance of these responses in such patients
8 remains unclear. Consequently, primary systemic vasculitis patients receiving anti-CD20
9 therapies may still be vulnerable to severe SARS-CoV-2 infection even if they develop
10 antibodies following primary vaccination, particularly given the emergence of variants with
11 humoral immune escape properties.

12 We have recently developed a novel immunoassay, microfluidic antibody affinity profiling
13 (MAAP), for in solution quantification of the fundamental parameters of the antibody
14 response, namely affinity and concentration, directly in serum(25) and used it to characterise
15 antibody profiles against wildtype (WT) SARS-CoV-2 in convalescent sera(26) and to study
16 the role of cross-reactivity as a consequence of memory reactivation after acute SARS-CoV-2
17 infection(27). MAAP can distinguish samples containing low levels of high-affinity
18 antibodies from samples with high levels of low-affinity antibodies, which would otherwise
19 exhibit the same EC₅₀ (half-maximal effective concentration) using an ELISA-based
20 technique(26, 27). Thus, MAAP may allow for a more granular assessment of antibody
21 responses following antigen exposure and provide insights into the potency of the humoral
22 response against emerging variants of concern. Nevertheless, a recent study exploring
23 antibody profiles in pre-Omicron sera from largely immunocompetent patients with a variety
24 of antigenic exposures to SARS-CoV-2 antigens (including after one or more doses of WT
25 vaccine or after infection or both) showed similar antibody affinities against Omicron versus

1 WT or Delta Spike antigens, albeit the timing of serum sampling for antibody assessment in
2 this study was widely variable(28).

3 Several recently published studies have assessed humoral responses following booster
4 vaccination(s) among cohorts of patients with autoimmune/inflammatory conditions on anti-
5 CD20 therapies, which have included vasculitis patients(29-34), although few have examined
6 primary systemic vasculitis patients specifically(35-37). The primary aim of this study was to
7 perform in depth serological characterisation of antibody responses at pre-specified time
8 points after repeated vaccination (specifically after second and third doses) against SARS-
9 CoV-2 in pre-Omicron sera from Rituximab treated patients with primary systemic vasculitis.
10 Along with serological profiling using solid-phase and neutralisation assays, we capitalised
11 on our recently described microfluidics-based immunoassay to quantify antibody affinity and
12 concentration against wild-type (WT) versus Omicron strains of SARS-CoV-2. We
13 subsequently performed antibody profiling at equivalent time points in a cohort of healthy
14 individuals after similar, repeated antigenic exposure to SARS-CoV-2. Finally, we compared
15 the serological response to repeated vaccination in Rituximab treated patients to that in
16 unvaccinated, convalescent patients after a single exposure to WT SARS-CoV-2 infection.
17 We found suboptimal humoral immunity even after repeated vaccination in Rituximab treated
18 patients and highlight the role of quantitative assessment of serum antibody affinity and
19 concentration in monitoring anti-viral immunity, viral escape, and the evolution of the
20 humoral response.

21

1 Methods

2 *Cohort Description*

3 Patients with primary systemic vasculitides were recruited from a prospective observational
4 cohort study investigating SARS-CoV-2 vaccine responses among renal populations at the
5 Department of Nephrology at Cambridge University Hospitals NHS Foundation Trust (CUH)
6 (ethics reference: 20/EM/0180), as previously described (38). Patients receiving IVIg or
7 plasma exchange were excluded as potential confounders of vaccine responses. Samples from
8 the health care worker cohort were part of the asymptomatic staff screening programme at
9 CUH, as previously described(39). All staff members were invited to participate in the
10 serological screening programme and provided written informed consent (NIHR BioResource
11 - COVID-19 Research cohort; ethics reference: 17/EE/0025, IRAS ID: 220277). The study
12 participants in the convalescent patient cohort were recruited between March 2020 and July
13 2020 from patients attending CUH with nucleic acid confirmed diagnosis of COVID-19
14 (ethics reference: 17/EE/0025), as previously described(40). All participants provided
15 informed consent.

16 Blood samples were taken at approximately 4 to 6 weeks after each sensitisation/vaccination
17 event (1A, 2A or 3A) with flexibility to align with routine clinical tests and access to blood
18 testing facilities wherever possible. Blood samples for the convalescent cohort were taken at
19 the time points specified (1A: one month and 1B: three months from diagnosis of COVID-
20 19). Clinical data collected from electronic medical records and patient interviews included
21 baseline demographics, changes to immunosuppressive medication over time, and data on
22 episodes of SARS-CoV-2 infection.

1 *Fluorescent labelling of proteins*

2 Recombinant SARS-CoV-2 Spike RBD proteins from WT (#40592-V08H) and Omicron
3 (B.1.1.529; #40592-V08H121) strains were purchased from Sino Biological and labelled with
4 AlexaFluor 647 as previously described(25). In brief, 100 μ g SARS-CoV-2 RBD protein was
5 re-suspended in H₂O and mixed with NaHCO₃ (pH 8.3) buffer to a final concentration of
6 100mM. DMSO-reconstituted AlexaFluorTM 647 N-hydroxysuccinimidyl ester
7 (ThermoFisher) was added at a 3-fold molar excess and the reaction was incubated at room
8 temperature for 1h. The reaction mixture underwent size-exclusion chromatography in PBS,
9 pH 7.4 using an ÄKTA pure system and a Superdex 200 Increase 10/300 column (Cytiva) to
10 separate the labelled protein from the free fluorophore. Labelled proteins fractions were
11 pooled, concentrated using an Amicon Ultra-0.5 10K centrifugal filter device (Millipore) and
12 glycerol was added to a concentration of 10% (w/v) prior to snap freezing in LN₂ and storage
13 at -80°C. Upon thawing and before use, protein concentrations were quantified via Nanodrop
14 using the molar extinction coefficient.

15 *Antibody affinity and concentration measurements*

16 The affinity and concentration of anti-RBD antibodies within patient sera were determined
17 using Microfluidic antibody affinity profiling (MAAP)(26). The hydrodynamic radius (R_H) of
18 1nM-500 nM AlexaFluorTM 647-labelled Spike RBD proteins were measured in the presence
19 of MAAP buffer (PBS containing 5% human serum albumin (sigma), 10% (w/v) glycerol and
20 0.05% Tween-20) and varying concentrations (0-50%) of patient serum via microfluidic
21 diffusional sizing (MDS) using the Fluidity One-W or One-M instruments (Fluidic Analytic
22 Ltd.) after a one-hour incubation on ice. The background fluorescence within each diffused
23 and non-diffused microfluidic stream was subtracted from the MDS data for the specific
24 serum concentrations and Bayesian inference analysis was used to constrain the values of

1 affinity (K_D) and antibody binding sites ([Ab]), as previously described(25, 26). Serum
2 samples that enabled constrained K_D and [Ab] values to be measured (with both upper and
3 lower 95% confidence intervals) were considered quantifiable. Those that had an [Ab]/ K_D
4 ratio of >2 were labelled as fully quantifiable (Q), and those that had a [Ab]/ K_D of 1-2 were
5 considered to be at the border of sensitivity for full quantification (B; borderline). Samples
6 which yielded no measured increase in the RBD hydrodynamic radius after serum incubation
7 (N; non-binders) and/or those samples that yielded incomplete K_D and/or [Ab] bounds (U;
8 unquantifiable due to inability to fully constrain 95% confidence interval lower bounds for
9 both parameters) were deemed non-quantifiable and excluded from subsequent analysis.

10 *Luminex assay*

11 Serum antibody reactivity to SARS-CoV-2 WT Spike, RBD and nucleocapsid proteins was
12 assessed using a UKAS accredited Luminex platform, as previously reported(41). In brief,
13 patient serum diluted 1/100 was incubated for 1h at room temperature with WT Spike, RBD
14 or Nucleocapsid proteins covalently coupled to distinct carboxylated beads in a triplex assay.
15 The liquid phase was aspirated and beads were washed with 10mM PBS/0.05% Tween-20
16 three times before incubation with PE-conjugated anti-human IgG-Fc antibody
17 (Leinco/Biotrend) for 30 minutes. Beads were washed again as above and resuspended in
18 100 μ l PBS/Tween before being analysed on a Luminex analyser (Luminex/R&D Systems)
19 using Exponent Software V31. Specific binding of antibodies to each protein was reported as
20 the mean fluorescence intensity (MFI).

21 *Pseudotype neutralisation assay*

22 Sera were heat-inactivated at 56°C for 30 min, then frozen in aliquots at -80°C. Virus
23 neutralisation assays were performed on HEK293T cells that were transiently transfected
24 with ACE2 using a SARS-CoV-2 Spike pseudotyped virus expressing luciferase, as

1 previously described(42). Pseudotyped virus were prepared by transfection of HEK293T cells
2 using the Fugene HD transfection system (Promega), as previously described(42).
3 Pseudotyped virus was incubated with serial dilution of heat-inactivated human serum
4 samples in duplicate for 1h at 37°C. Virus-only and cell-only controls were included. Freshly
5 trypsinised HEK293T ACE2-expressing cells were added to each well. Following 48h
6 incubation in a 5% CO₂ environment at 37°C, luminescence was measured using the Bright-
7 Glo Luciferase assay system (Promega) and neutralization calculated relative to virus-only
8 controls. Neutralising antibody titres at 50% inhibition (ND₅₀) were calculated in GraphPad
9 Prism.

10 *Statistical analysis*

11 Statistical analyses were carried out using GraphPad Prism v9.5.0 and in *R* version 4.2.3.
12 Comparison of paired datasets was done using the Wilcoxon matched paired-signed ranked
13 test to track the trending pattern between the paired samples and the Mann-Whitney U test
14 was used to compare distributions between two groups. Multiple group differences were
15 analysed using Kruskal-Wallis tests and pairwise differences across groups were examined
16 using the Dunn's test, with Benjamini-Hochberg corrections to account for potential false
17 discovery from multiple comparisons. Linear regression models were optimised to assess
18 relationships between variables where indicated. All p-values are two-tailed where ns>0.05,
19 *≤0.05, **≤0.01, ***≤0.001, ****≤0.0001.

20 For visualisation, scatter, violin, and boxplots were generated using the ggplot2 package
21 (version 3.4.2). Contour lines were superimposed upon a scatter plot using the geom_hdr
22 function provided by the ggdensity package (version 1.0.0). Correlation values, including
23 both Pearson and Spearman coefficients, were determined via the cor.test function of the stats
24 package. These values were then annotated on the plots using the annotate function inherent

1 to ggplot2. The summary heatmap was created with the ComplexHeatmap package (version
2 2.15.4).

3 *Data availability statement*

4 All data generated in this study are available as supplementary information.

5

1 **Results**

2 *Anti SARS-CoV-2 antibody profiling in Rituximab treated vasculitis patients*

3 We identified a cohort of 14 patients with primary systemic vasculitis treated with Rituximab
4 (RTX cohort) who had been recruited in a prospective observational cohort study
5 investigating SARS-CoV-2 vaccine responses among renal populations(38) and had paired
6 samples, collected at pre-specified time points, after the first, second and third vaccine doses.
7 The patient demographics are summarised in supplementary Table 1. The majority of patients
8 (79%) had Rituximab within 12 months prior to first vaccine dose and 64% had additional
9 Rituximab between vaccine doses. Serological responses to wild-type SARS-CoV-2 Spike
10 and RBD, as assessed by an accredited Luminex immunoassay 4-6 weeks after each vaccine
11 dose, are shown in Figure 1. Overall, 57% of the cohort showed a positive anti-Spike
12 response (median [range] MFI: 3,958 [59-22,509]) and 14% a positive anti-RBD response
13 (median [range] MFI: 115 [46-2,437]) after the first vaccine dose. Seroconversion and
14 Luminex MFI values increased significantly after the second vaccine dose, both against Spike
15 (100% positive; median [range] MFI: 27,713 [9,047-32,716]; p<0.0001 Mann-Whitney test)
16 and RBD (71% positive; median [range] MFI: 5,301 [33-31,509]; p=0.0384 Mann-Whitney
17 test), and remained stable after the third vaccine dose (100% anti-Spike positive; median
18 [range] MFI: 27,356 [2,398-32,662]; p=0.5007 and 64% anti-RBD positive; median [range]
19 MFI: 19,741 [127-32,331]; p=0.2915 between second and third vaccine doses; Mann-
20 Whitney test). Notably, four patients showed consistently negative anti-RBD responses, and
21 42% of sera with significant anti-Spike antibody reactivity (n=33) were negative against
22 SARS-CoV-2 RBD (n=14). Patients who received additional Rituximab between second and
23 third vaccine doses (n=6) did not have significantly different antibody responses compared to
24 those who did not (median [range] MFI after third vaccine: anti-Spike; 32,552 [9,047-32,716])

1 versus 27,356 [13984-32,662], p=0.5368, anti-RBD; 19,176 [33-31,501.8] versus 26,931
2 [136-32,331], p=0.4286, Mann-Whitney tests).

3 Neutralising antibodies against WT were detectable in 50% of patients both after the second
4 and third vaccine doses with, overall, similar 50% neutralising dose titres (ND₅₀) between the
5 two time points (median [range] ND₅₀ of 207 [20-2,254] versus 240 [20-7,468], p=0.5890
6 Mann-Whitney test). Nevertheless, individual patient responses after vaccination were
7 variable with neutralising titres increasing in six patients, decreasing in three patients,
8 whereas a further five patients did not develop neutralising antibodies after three vaccine
9 doses (Figure 2A). To provide a more in depth analysis of serological responses in these
10 patients, we further characterised anti-RBD antibodies by MAAP. Consistent with Luminex,
11 MAAP showed that the affinity (K_D) and concentration ([Ab]) of antibodies against WT RBD
12 did not change significantly between the second and third vaccine doses (Figure 2B-C). All
13 neutralising sera were quantifiable by MAAP whereas non-neutralising sera could not be
14 quantified either due to undetectable/low anti-RBD antibody levels (n=10, RBD MFI 33-
15 3,440) or the inability to effectively constrain MAAP parameters (n=3, RBD MFI 5,301-
16 19,741; Supplementary Figure 1 and Supplementary Table 2; one non-neutralising serum had
17 a missing MFI and showed minimal binding on MAAP). Overall, the affinity of quantifiable
18 anti-WT RBD antibodies ranged widely from 2.3 nM to 44.8 nM and in patients with
19 increasing neutralisation titres after the third vaccine dose, this was driven predominantly by
20 an increase in antibody concentration rather than improvement in affinity.

21 Analysis of serum antibody reactivity against the Omicron variant showed that only 3/14
22 (21%) and 4/14 (29%) patients developed neutralising antibodies after the second and third
23 vaccine doses, respectively. Similar to WT, individual patient responses varied although more
24 patients had measurable Omicron anti-RBD antibodies after the third vaccine dose (seven
25 patients had an improved and three patients a worse response to Omicron RBD), as

1 determined by MAAP (Figure 2 D-F and Supplementary Table 2). Overall, the affinity of
2 anti-Omicron RBD antibodies varied from 9.7-38.8 nM and their concentration from 56.5-
3 1,080 nM with no significant difference in either parameter between the two time points.
4 Importantly, there was decreased neutralisation capacity against Omicron compared to WT
5 both after the second and third vaccine doses (Figure 3A-C). MAAP analysis showed that this
6 difference was driven by significantly weaker antibody affinity to the Omicron versus WT
7 RBD (median [range] KD: 21.6 [9.7-38.8] nM vs 4.6 [2.3-44.8] nM respectively, p=0.0004
8 Wilcoxon paired ranked test) rather than by differences in antibody concentration (median
9 [range] [Ab]: 171 [56.5-1,080] nM vs 177 [43.7-952] nM respectively, p=0.2412, Wilcoxon
10 paired ranked test), and this was consistent at both time points (Supplementary Figure 2).
11 Overall, 14 (50%) samples had no neutralisation against either variant, whereas five patients
12 did not develop neutralising antibodies at either timepoint. Taken together, the above results
13 demonstrate that Rituximab treated patients developed widely variable antibody responses to
14 SARS-CoV-2 after repeated vaccination which, when quantifiable by MAAP, varied by 20-
15 fold in affinity. Overall, neutralising antibody responses were often absent even after three
16 vaccine doses; when present, neutralisation capacity was significantly weaker against
17 Omicron versus WT SARS-CoV-2 strains and this difference was driven by the weaker
18 affinity of vaccine induced antibodies against the Omicron strain.

19 *Anti-SARS-CoV-2 antibody profiling in healthy individuals versus Rituximab treated patients*
20 We next hypothesised that the quality of the antibody response would vary significantly in
21 healthy individuals compared to Rituximab treated patients following antigenic exposure to
22 SARS-CoV-2. To investigate this, we profiled antibody responses in health care workers
23 (HCW) recruited at Cambridge University Hospital who, similar to the vasculitis cohort, had
24 three exposures to SARS-CoV-2 antigen, consisting of an asymptomatic infection to SARS-
25 CoV-2 prior to the emergence of the Omicron variant and two subsequent vaccine doses (see

1 methods and supplementary Table 1). Antibody profiling was performed at 4 weeks after the
2 third exposure (second vaccine dose). Luminex analyses showed significantly higher
3 antibody reactivity to WT Spike and RBD in HCW versus Rituximab treated patients
4 (Supplementary Figure 3, Supplementary Table 4). Similar to Rituximab treated patients,
5 neutralisation titres in HCW were significantly higher against the WT versus the Omicron
6 variant. Further profiling by MAAP suggested this difference was driven by the fact only a
7 fraction of high affinity serum antibodies recognised the Omicron RBD (Supplementary
8 Figure 3). Compared to Rituximab treated patients (Figure 4), MAAP quantifiable antibodies
9 to WT SARS-CoV-2 in the HCW cohort were of higher concentration (median [range] [Ab]
10 of 236.5 [49.5-952] nM vs 646 [233-2,110] nM, respectively, $p=0.0018$ Mann-Whitney test)
11 but of similar affinity (median [range] K_D of 4.6 [2.3-44.8] nM vs 4.7 [1.2-19.0] nM,
12 respectively, $p=0.5825$ Mann-Whitney test) underpinning the higher neutralisation titres in
13 the HCW cohort (median [range] ND_{50} of 49 [20-7,468]) versus 2,522 [864-7,297], $p=0.0004$
14 Mann-Whitney test; Figure 4). Neutralisation titres against the Omicron strain were also
15 higher in HCW versus Rituximab treated patients (median [range] ND_{50} of 221.5 [24.63-
16 1,225] versus 20 [20-648.7], respectively, $p=0.003$ Mann-Whitney test; Figure 4) but this was
17 driven by higher affinity anti-Omicron RBD antibodies in the HCW cohort (median [range]
18 K_D : 1.05 [0.45-1.84] nM vs 20.25 [13.2-38.8] nM, $p=0.0002$ Mann-Whitney test). Taken
19 together, our results confirm the previously reported impaired antibody responses to SARS-
20 CoV-2 variants of concern in Rituximab treated, immunosuppressed patients compared to
21 healthy individuals and, through MAAP analysis, highlight the significance of the
22 fundamental parameters of the antibody response, namely antibody affinity and
23 concentration, to anti-viral immunity and virus escape.

1 *Evolution of antibody response to SARS-CoV-2 after infection and vaccination*

2 In the microfluidic-based antibody profiling of the Rituximab patient cohort described above,

3 we could not detect evidence of affinity maturation in peripheral blood samples collected

4 after the second compared to third vaccine doses, despite a median of 185 days (range 141-

5 224 days) between the two time points. To investigate whether this observation was specific

6 to the Rituximab treated patients, we next examined the quality of the humoral response after

7 WT SARS-CoV-2 infection in patients during the first wave of the COVID-19 pandemic

8 using samples collected at one and three months post infection (see methods). The

9 demographic characteristics of this cohort (n=30) are shown in supplementary Table 1. As

10 shown in Figure 5, we observed wide variation in affinity (K_D range 2.07-34.0 nM) and

11 concentration (range 7.1-1,120 nM) of the antibody responses to WT RBD at both time

12 points. As expected, there was a significant decrease in antibody concentration over time

13 (median [range]: 55.6 [7.1-269] nM at 3 months vs 169 [13-1,120] nM at 1 month post-

14 infection, $p=0.0034$, Wilcoxon paired ranked test) and an associated decrease in

15 neutralisation capacity (median [range] ND_{50} of 131 [20-7,983] versus 280 [20-14,580],

16 respectively, $p=0.0296$, Wilcoxon paired ranked test). Nevertheless, we were able to detect

17 evidence of affinity maturation over the same time period, as demonstrated by a decrease in

18 anti-RBD dissociation constant in the majority of patients (median [range] K_D : 6.6 [2.1-14.6]

19 nM at 3 months vs 9.4 [2.1-34] nM at 1 month post-infection, $p=0.0244$, Wilcoxon paired

20 ranked test). Luminex analysis of antibody reactivity to WT Spike and RBD showed

21 significantly higher responses at one month after infection in the convalescent cohort

22 compared to one month after the first vaccine dose in the Rituximab cohort; these antibodies

23 in Rituximab treated patients reached similar levels to those in the convalescent cohort after

24 the second and third vaccine doses (supplementary Figure 4D-E). Comparison of the

25 convalescent cohort at one month post-infection with the Rituximab treated patient cohort at

1 equivalent time points after the second and third vaccine dose showed similar neutralisation
2 titres against WT SARS-CoV-2 despite exposure to only a single sensitisation event (Figure
3 6). Corroborating these findings, quantification of WT anti-RBD responses by MAAP
4 showed similar antibody affinity and concentration after the second and third vaccine dose in
5 Rituximab treated patients compared to those in post-infection convalescent patients (Figure
6 6B-C).

7 *Multidimensional assessment of antibody fingerprints (concentration and affinity) with*
8 *clinical parameters at the individual patient level*

9 To provide a global perspective of antibody affinity/concentration profiles against WT and
10 Omicron variants, we created integrated 2D-density contour plots incorporating MAAP data
11 obtained from the above three patient groups (Rituximab treated vasculitis patients ~1 month
12 after the third vaccine dose vs health care workers ~1 month after the third sensitisation event
13 vs COVID-19 convalescent patients ~1 month post-infection). As shown in Figure 7, HCW
14 clustered separately (high affinity and high [Ab] profiles), whereas the density
15 representations for Rituximab treated and convalescent patients were wider and largely
16 overlapping. As discussed above, a left shift of antibody profiles to the Omicron variant was
17 apparent in Rituximab patients with significantly lower affinity compared to anti-Omicron
18 profiles in the HCW cohort. The relationship of antibody fingerprints with clinically relevant
19 parameters showed that the $K_D \times [Ab]$ product was similar between female and male patients,
20 whereas a weak negative correlation was noted with increasing age for anti-WT antibody
21 profiles (Spearman correlation coefficient $\rho=-0.67$, $p=0.0012$; Figure 7B-C). For
22 convalescent patients, the $K_D \times [Ab]$ product tended to be higher in patients with more severe
23 disease (Figure 7D).

24 We next incorporated serological parameters (MAAP affinity/concentration, Luminex MFI,
25 ND₅₀) with relevant immunological and demographic variables (SARS-CoV-2 variant,

1 vaccine dose, patient cohort, age, sex and ethnic background) to provide a comprehensive
2 multidimensional assessment at the single-individual level (Figure 8A), which highlighted the
3 strength of the anti-SARS-CoV-2 response (higher ND₅₀, [Ab], Luminex anti-Spike and anti-
4 RBD MFI) in healthy individuals, compared to Rituximab treated and convalescent patients.
5 We also related antibody WT SARS-CoV-2 serological read-outs obtained from
6 neutralisation, MAAP and Luminex assays, which showed a strong correlation between ND₅₀
7 and antibody concentration or ND₅₀ and Luminex RBD MFI (Spearman correlation
8 coefficient $\rho=0.74$, $p=8.1\times10^{-12}$ and $\rho=0.81$, $p=5.5\times10^{-24}$, respectively; Figure 8B-C) but no
9 relationship between ND₅₀ or Luminex RBD MFI with antibody affinity (supplementary
10 Figure 5). These observations suggest that neutralisation and solid-phase Luminex assays
11 primarily reflect antibody concentrations (supplementary Figure 5C) rather than affinities for
12 MAAP quantifiable samples analysed here.

13

14

1 Discussion

2 In this study, primary systemic vasculitis patients treated with Rituximab had significantly
3 impaired humoral immune responses compared to healthy individuals after three exposures to
4 SARS-CoV-2 antigens, demonstrated by lower anti-Spike and -RBD antibody levels and
5 lower neutralisation titres against both wildtype and Omicron variants. Despite an
6 incremental increase in antibody levels after the second vaccine dose, no further enhancement
7 of the response was noted after a third dose. Correspondingly, after a third vaccine dose,
8 approximately half and two thirds of Rituximab patients had no detectable neutralising
9 antibodies against WT and Omicron, respectively. Relative to unvaccinated convalescent
10 individuals, Rituximab treated patients had similar anti-Spike and anti-RBD antibody levels
11 and similar (albeit numerically lower) neutralisation titres to WT SARS-CoV-2, despite two
12 more exposures to SARS-CoV-2 antigen. Antibodies produced by Rituximab treated patients
13 varied by 20-fold of magnitude in affinity, and the difference in neutralisation capacity
14 between Omicron and WT SARS-CoV-2 was driven by the weaker affinity of vaccine
15 induced antibodies against the Omicron variant. By contrast, healthy individuals with hybrid
16 immunity in the form of previous infection and two vaccinations produced a broader, high
17 concentration antibody response as profiled using MAAP, a subset of which recognised
18 Omicron RBD with higher affinity than antibodies in Rituximab treated patients, likely
19 underpinning the more effective neutralisation capacity against Omicron in this group
20 compared to Rituximab treated patients. Finally, we demonstrate that MAAP can assess the
21 evolution of humoral immune responses by direct measurement of polyclonal antibody
22 affinity in serum, without the need for antigen-specific B cell isolation and antibody
23 sequencing or measurement of antibody dissociation kinetics in solid-phase assays that can be
24 perturbed by avidity-driven interactions(43-45). Accordingly, we detected evidence of
25 affinity maturation within three months from primary infection in convalescent patient sera

1 despite a relative decrease in anti-RBD antibody concentration. This was not evident in
2 Rituximab treated patients even after a third vaccine dose.
3 Our findings of impaired humoral immune responses after a third SARS-CoV-2 vaccine dose
4 in our primary systemic vasculitis patient cohort receiving anti-CD20 therapies are in
5 agreement with the recently published literature, although we are unaware of any other
6 groups who have quantified these using a combination of neutralisation assays and MAAP. A
7 recently published study of 21 patients with antineutrophil cytoplasmic antibody vasculitis
8 (AAV) showed that none of their 8 Rituximab-treated patients had detectable neutralising
9 antibodies to B.1.617.2 (Delta) following a third dose of BNT162b(35). By contrast, in a
10 small cohort of 15 AAV patients on Rituximab who received a third vaccine dose, 7/15
11 (46.7%) developed measurable IgG antibodies to the S1 subunit of the SARS-CoV-2 Spike
12 protein, although the neutralisation capacity of these antibodies was not assessed(36).
13 Humoral immune responses following a third vaccine dose among patients on anti-CD20
14 therapies with other autoimmune/inflammatory conditions are also impaired compared to
15 similar patients on other immunosuppressive agents and healthy controls(14-16, 31, 46, 47).
16 Additionally, among patients on anti-CD20 therapies who had not seroconverted following
17 primary vaccination, a third dose led to seroconversion rates of approximately 15-60%(29,
18 32-34, 48, 49). Another small study demonstrated an inverse correlation between Rituximab
19 dose and seroconversion and that antibody levels persisted after a subsequent dose of
20 Rituximab among those who had already seroconverted(50). A fall in antibody levels
21 following a dose of Rituximab between a second and third SARS-CoV-2 vaccine dose was
22 recently reported, although neutralisation capacity was preserved in seroconverted
23 patients(51). In an open-label study of a fourth dose of mRNA vaccine among Rituximab
24 treated patients, predominantly those with rheumatoid arthritis or connective tissue diseases,

1 a moderate improvement in seroconversion from 33% to 58% was demonstrated after the
2 fourth dose(30).

3 Among the patients in our cohort with detectable anti-Spike antibody responses following
4 SARS-CoV-2 vaccination, the impact of Rituximab on B cell populations, particularly
5 memory B cells, may be of relevance to their impaired neutralising ability and affinity
6 maturation compared to healthy controls. Memory B cells, in addition to enabling anamnestic
7 antibody responses, also allow for the development of reactive humoral responses in the
8 event of exposure to variant pathogens(52, 53). After vaccination, SARS-CoV-2 specific
9 memory B cells have been shown to persist for several months, even after antibody titres
10 have declined(54). Furthermore, a third dose of mRNA vaccine has been shown to increase
11 the breadth and potency of memory B cells and their antibody responses, including against
12 Omicron(54, 55). Following Rituximab treatment, memory B cells are often the last to
13 reconstitute among peripheral blood B cell populations(56-59), a process that can take up to
14 several years(57). Additionally, Rituximab treatment has also been associated with delays in
15 the acquisition of somatic hypermutations among repopulated memory B cells(60). Recent
16 data suggest that the presence of detectable peripheral circulating B cells is critical for
17 seroconversion following vaccination among Rituximab treated patients(29), with SARS-
18 CoV-2 specific memory B cell and plasmablast populations positively correlating with
19 antibody titres and neutralisation(61). Furthermore, a preponderance of naïve and transitional
20 B cells among Rituximab-treated patients prior to vaccination, indicative of early B cell
21 reconstitution, was found to be associated with adequate humoral immune responses
22 following vaccination(62). In support of this, improved serological responses after SARS-
23 CoV-2 vaccination have been associated with increasing time since the last Rituximab dose,
24 particularly if this interval is more than six months(63, 64). Notably in our cohort, 36% of
25 patients received Rituximab within 6 months from the first vaccine dose and 64% received an

1 additional Rituximab dose between first and third vaccine dose potentially accounting for the
2 lack of improvement in the humoral response and the absence of affinity maturation between
3 second and third vaccine doses.

4 A strength of our study is that we prospectively evaluated antibody responses at specific time
5 points in a relatively understudied cohort of primary systemic vasculitis patients who are
6 particularly vulnerable to both poorer clinical outcomes from COVID-19 and impaired
7 humoral immune responses after vaccination. Importantly, by quantifying antibody affinity
8 and concentration directly in serum, together with data from solid-phase Luminex and
9 neutralisation assays, we were able to provide additional insights into the quality of the
10 immune response against WT and Omicron variants after vaccination in Rituximab treated
11 patients. Additionally, we provide a comparative assessment with the humoral response at
12 equivalent time points in non-immunocompromised cohorts after infection/vaccination and
13 after infection only. In this regard, this is the largest study to date using a novel microfluidic
14 assay to quantify SARS-CoV-2 antibody affinity and concentration in serum samples. The
15 limitations of our investigations reside in the relatively small number of Rituximab treated
16 patients included in the study and the lack of a pre-Omicron control group of previously
17 uninfected healthy individuals with three vaccinations. It would have also been informative to
18 incorporate analysis on antigen-specific T cell and B cell mediated cellular immunity and
19 how this may relate to the observed serological response. Finally, the limits of sensitivity of
20 the MAAP assay should be noted. These reflect the lower limit of labelled antigen
21 concentration that can be employed owing to intrinsic background serum fluorescence and
22 the fact that antibody affinity and concentration cannot be constrained in samples with low
23 concentration and/or low affinity antibodies (e.g. where $[Ab] < K_D$)(25).

24 In conclusion, our results confirm and enrich the previously reported observations of
25 impaired humoral immune responses to SARS-CoV-2, including variants of concern, in

1 Rituximab treated, immunosuppressed patients compared to healthy individuals. Through the
2 addition of MAAP analysis, we highlight the significance of the fundamental parameters of
3 the antibody response, namely antibody affinity and concentration, to anti-viral immunity and
4 viral escape. Consequently, should our results be replicated, we would caution against
5 interpreting the presence of solid-phase assay detected anti-Spike antibodies following
6 vaccination as providing evidence of immune protection against SARS-CoV-2 infection,
7 particularly among patients on anti-CD20 therapies.

8
9

1 *Acknowledgements*

2 This study was funded in part by the University of Cambridge's Wellcome COVID-19 Rapid
3 Response DCF (RG93172 to VK). We acknowledge funding support from the National
4 Institute for Health Research Blood and Transplant Research Unit (NIHR BTRU, Grant
5 number: NIHR203332) in Organ Donation and Transplantation at the University of
6 Cambridge in collaboration with Newcastle University and in partnership with NHS Blood
7 and Transplant (NHSBT). The views expressed are those of the authors and not necessarily
8 those of the National Health Service, the National Institute for Health Research, the
9 Department of Health or National Health Service Blood and Transplant. VK acknowledges
10 funding from an NIHR Fellowship (PDF-2016-09-065) and as a Paul I. Terasaki Scholar. RS
11 acknowledges funding from Addenbrooke's Charitable Trust and Vasculitis UK. RK and IM
12 are funded by the Wellcome Trust [203151/Z/16/Z]. We thank all the patients and health care
13 workers who consented to take part in this study. We also thank the NIHR Cambridge
14 Biomedical Research Centre for support with sample recruitment. For the purpose of open
15 access, the authors applied a CC BY public copyright licence to all versions of the manuscript
16 arising from this submission.

17 *Author contributions*

18 AP, RS, TPJK and VK contributed to conception and design of the study. AP, SM, GM and
19 CKX performed MAAP experiments and analysed the respective data. MXC-X, RJ, JRB and
20 DJC collected and annotated patient samples. MH and IGG performed neutralisation studies
21 and RD performed Luminex analyses. AP, RK and IIM performed statistical analyses. MXC-
22 X, AP and VK wrote the manuscript. All authors read and revised the article and approved
23 the submitted version.

24 *Declaration of interests*

1

2

1 References

- 2 1. Andersen KM, Bates BA, Rashidi ES, Olex AL, Mannon RB, Patel RC, et al. Long-term
3 use of immunosuppressive medicines and in-hospital COVID-19 outcomes: a retrospective
4 cohort study using data from the National COVID Cohort Collaborative. *Lancet Rheumatol.*
5 2022;4(1):e33-e41.
- 6 2. Strangfeld A, Schafer M, Gianfrancesco MA, Lawson-Tovey S, Liew JW, Ljung L, et al.
7 Factors associated with COVID-19-related death in people with rheumatic diseases: results
8 from the COVID-19 Global Rheumatology Alliance physician-reported registry. *Ann Rheum
9 Dis.* 2021;80(7):930-42.
- 10 3. Akiyama S, Hamdeh S, Micic D, Sakuraba A. Prevalence and clinical outcomes of
11 COVID-19 in patients with autoimmune diseases: a systematic review and meta-analysis.
12 *Ann Rheum Dis.* 2021;80(3):384-91.
- 13 4. Agrawal U, Bedston S, McCowan C, Oke J, Patterson L, Robertson C, et al. Severe
14 COVID-19 outcomes after full vaccination of primary schedule and initial boosters: pooled
15 analysis of national prospective cohort studies of 30 million individuals in England, Northern
16 Ireland, Scotland, and Wales. *Lancet.* 2022;400(10360):1305-20.
- 17 5. Schietzel S, Anderegg M, Limacher A, Born A, Horn MP, Maurer B, et al. Humoral and
18 cellular immune responses on SARS-CoV-2 vaccines in patients with anti-CD20 therapies: a
19 systematic review and meta-analysis of 1342 patients. *RMD Open.* 2022;8(1).
- 20 6. Galmiche S, Luong Nguyen LB, Tartour E, de Lamballerie X, Wittkop L, Loubet P, et al.
21 Immunological and clinical efficacy of COVID-19 vaccines in immunocompromised
22 populations: a systematic review. *Clin Microbiol Infect.* 2022;28(2):163-77.
- 23 7. Ferri C, Ursini F, Gragnani L, Raimondo V, Giuggioli D, Foti R, et al. Impaired
24 immunogenicity to COVID-19 vaccines in autoimmune systemic diseases. High prevalence of
25 non-response in different patients' subgroups. *J Autoimmun.* 2021;125:102744.
- 26 8. UK Health Security Agency. COVID-19: the green book, chapter 14a The Green
27 Book2022.
- 28 9. World Health Organization. Good practice statement on the use of second booster
29 doses for COVID-19 vaccines. 2022 11/08/2022.
- 30 10. Centres for Disease Control and Prevention (CDC). COVID-19 Vaccines for People
31 Who Are Moderately or Severely Immunocompromised 2022 [updated 09/12/2022].
32 Available from: <https://www.cdc.gov/coronavirus/2019-ncov/vaccines/recommendations/immuno.html>.
- 34 11. Stevens KI, Frangou E, Shin JIL, Anders HJ, Bruchfeld A, Schonermanck U, et al.
35 Perspective on COVID-19 vaccination in patients with immune-mediated kidney diseases:
36 consensus statements from the ERA-IWG and EUVAS. *Nephrol Dial Transplant.*
37 2022;37(8):1400-10.
- 38 12. Lee A, Wong SY, Chai LYA, Lee SC, Lee MX, Muthiah MD, et al. Efficacy of covid-19
39 vaccines in immunocompromised patients: systematic review and meta-analysis. *BMJ.*
40 2022;376:e068632.
- 41 13. Vijenthira A, Gong I, Betschel SD, Cheung M, Hicks LK. Vaccine response following
42 anti-CD20 therapy: a systematic review and meta-analysis of 905 patients. *Blood Adv.*
43 2021;5(12):2624-43.
- 44 14. Wieske L, van Dam KPJ, Steenhuis M, Stalman EW, Kummer LYL, van Kempen ZLE, et
45 al. Humoral responses after second and third SARS-CoV-2 vaccination in patients with

1 immune-mediated inflammatory disorders on immunosuppressants: a cohort study. Lancet
2 Rheumatol. 2022;4(5):e338-e50.

3 15. Jyssum I, Kared H, Tran TT, Tveter AT, Provan SA, Sexton J, et al. Humoral and cellular
4 immune responses to two and three doses of SARS-CoV-2 vaccines in rituximab-treated
5 patients with rheumatoid arthritis: a prospective, cohort study. Lancet Rheumatol.
6 2022;4(3):e177-e87.

7 16. Firinu D, Fenu G, Sanna G, Costanzo GA, Perra A, Campagna M, et al. Evaluation of
8 humoral and cellular response to third dose of BNT162b2 mRNA COVID-19 vaccine in
9 patients treated with B-cell depleting therapy. J Autoimmun. 2022;131:102848.

10 17. Cromer D, Steain M, Reynaldi A, Schlub TE, Wheatley AK, Juno JA, et al. Neutralising
11 antibody titres as predictors of protection against SARS-CoV-2 variants and the impact of
12 boosting: a meta-analysis. Lancet Microbe. 2022;3(1):e52-e61.

13 18. Cheng SMS, Mok CKP, Leung YWY, Ng SS, Chan KCK, Ko FW, et al. Neutralizing
14 antibodies against the SARS-CoV-2 Omicron variant BA.1 following homologous and
15 heterologous CoronaVac or BNT162b2 vaccination. Nat Med. 2022;28(3):486-9.

16 19. Bowen JE, Addetia A, Dang HV, Stewart C, Brown JT, Sharkey WK, et al. Omicron
17 spike function and neutralizing activity elicited by a comprehensive panel of vaccines.
18 Science. 2022;377(6608):890-4.

19 20. Hachmann NP, Miller J, Collier AY, Ventura JD, Yu J, Rowe M, et al. Neutralization
20 Escape by SARS-CoV-2 Omicron Subvariants BA.2.12.1, BA.4, and BA.5. N Engl J Med.
21 2022;387(1):86-8.

22 21. Willett BJ, Grove J, MacLean OA, Wilkie C, De Lorenzo G, Furnon W, et al. SARS-CoV-
2 Omicron is an immune escape variant with an altered cell entry pathway. Nat Microbiol.
23 2022;7(8):1161-79.

25 22. McCallum M, Walls AC, Sprouse KR, Bowen JE, Rosen LE, Dang HV, et al. Molecular
26 basis of immune evasion by the Delta and Kappa SARS-CoV-2 variants. Science.
27 2021;374(6575):1621-6.

28 23. Kent SJ, Khouri DS, Reynaldi A, Juno JA, Wheatley AK, Stadler E, et al. Disentangling
29 the relative importance of T cell responses in COVID-19: leading actors or supporting cast?
30 Nat Rev Immunol. 2022;22(6):387-97.

31 24. Wherry EJ, Barouch DH. T cell immunity to COVID-19 vaccines. Science.
32 2022;377(6608):821-2.

33 25. Schneider MM, Scheidt T, Priddey AJ, Xu CK, Hu M, Meisl G, et al. Microfluidic
34 antibody affinity profiling of alloantibody-HLA interactions in human serum. Biosens
35 Bioelectron. 2023;228:115196.

36 26. Schneider MM, Emmenegger M, Xu CK, Condado Morales I, Meisl G, Turelli P, et al.
37 Microfluidic characterisation reveals broad range of SARS-CoV-2 antibody affinity in human
38 plasma. Life Sci Alliance. 2022;5(2).

39 27. Denninger V, Xu CK, Meisl G, Morgunov AS, Fiedler S, Ilsley A, et al. Microfluidic
40 Antibody Affinity Profiling Reveals the Role of Memory Reactivation and Cross-Reactivity in
41 the Defense Against SARS-CoV-2. ACS Infect Dis. 2022;8(4):790-9.

42 28. Emmenegger M, Fiedler S, Brugger SD, Devenish SRA, Morgunov AS, Ilsley A, et al.
43 Both COVID-19 infection and vaccination induce high-affinity cross-clade responses to SARS-
44 CoV-2 variants. iScience. 2022;25(8):104766.

45 29. Ammitzboll C, Kragh Thomsen M, Bogh Andersen J, Jensen JMB, From Hermansen
46 ML, Dahl Johannsen A, et al. Rituximab-treated rheumatic patients: B-cells predict

1 seroconversion after COVID-19 boost or revaccination in initial vaccine non-responders.
2 Rheumatology (Oxford). 2022.
3 30. Mrak D, Simader E, Sieghart D, Mandl P, Radner H, Perkmann T, et al.
4 Immunogenicity and safety of a fourth COVID-19 vaccination in rituximab-treated patients:
5 an open-label extension study. Ann Rheum Dis. 2022.
6 31. Sidler D, Born A, Schietzel S, Horn MP, Aeberli D, Amsler J, et al. Trajectories of
7 humoral and cellular immunity and responses to a third dose of mRNA vaccines against
8 SARS-CoV-2 in patients with a history of anti-CD20 therapy. RMD Open. 2022;8(1).
9 32. Bitoun S, Avouac J, Henry J, Ghossan R, Al Tabaa O, Belkhir R, et al. Very low rate of
10 humoral response after a third COVID-19 vaccine dose in patients with autoimmune
11 diseases treated with rituximab and non-responders to two doses. RMD Open. 2022;8(1).
12 33. Bonelli M, Mrak D, Tobudic S, Sieghart D, Koblischke M, Mandl P, et al. Additional
13 heterologous versus homologous booster vaccination in immunosuppressed patients
14 without SARS-CoV-2 antibody seroconversion after primary mRNA vaccination: a
15 randomised controlled trial. Ann Rheum Dis. 2022;81(5):687-94.
16 34. Simon D, Tascilar K, Fagni F, Schmidt K, Kronke G, Kleyer A, et al. Efficacy and safety
17 of SARS-CoV-2 revaccination in non-responders with immune-mediated inflammatory
18 disease. Ann Rheum Dis. 2022;81(7):1023-7.
19 35. Speer C, Tollner M, Benning L, Klein K, Bartenschlager M, Nusshag C, et al. Third
20 COVID-19 vaccine dose with BNT162b2 in patients with ANCA-associated vasculitis. Ann
21 Rheum Dis. 2022;81(4):593-5.
22 36. Kant S, Azar A, Geetha D. Antibody response to COVID-19 booster vaccine in
23 rituximab-treated patients with anti-neutrophil cytoplasmic antibody-associated vasculitis.
24 Kidney Int. 2022;101(2):414-5.
25 37. Marty PK, Van Keulen VP, Erskine CL, Shah M, Hummel A, Stachowitz M, et al.
26 Antigen Specific Humoral and Cellular Immunity Following SARS-CoV-2 Vaccination in ANCA-
27 Associated Vasculitis Patients Receiving B-Cell Depleting Therapy. Frontiers in immunology.
28 2022;13:834981.
29 38. Smith RM, Cooper DJ, Doffinger R, Stacey H, Al-Mohammad A, Goodfellow I, et al.
30 SARS-CoV-2 vaccine responses in renal patient populations. BMC Nephrol. 2022;23(1):199.
31 39. Cooper DJ, Lear S, Watson L, Shaw A, Ferris M, Doffinger R, et al. A prospective study
32 of risk factors associated with seroprevalence of SARS-CoV-2 antibodies in healthcare
33 workers at a large UK teaching hospital. The Journal of infection. 2022;85(5):557-64.
34 40. Bergamaschi L, Mescia F, Turner L, Hanson AL, Kotagiri P, Dunmore BJ, et al.
35 Longitudinal analysis reveals that delayed bystander CD8+ T cell activation and early
36 immune pathology distinguish severe COVID-19 from mild disease. Immunity.
37 2021;54(6):1257-75.e8.
38 41. Xiong X, Qu K, Ciazyńska KA, Hosmillo M, Carter AP, Ebrahimi S, et al. A
39 thermostable, closed SARS-CoV-2 spike protein trimer. Nature Structural & Molecular
40 Biology. 2020;27(10):934-41.
41 42. Collier DA, De Marco A, Ferreira IATM, Meng B, Datir RP, Walls AC, et al. Sensitivity
42 of SARS-CoV-2 B.1.1.7 to mRNA vaccine-elicited antibodies. Nature. 2021;593(7857):136-41.
43 43. Bellusci L, Grubbs G, Zahra FT, Forgacs D, Golding H, Ross TM, et al. Antibody affinity
44 and cross-variant neutralization of SARS-CoV-2 Omicron BA.1, BA.2 and BA.3 following third
45 mRNA vaccination. Nature Communications. 2022;13(1):4617.

1 44. Cho A, Muecksch F, Schaefer-Babajew D, Wang Z, Finkin S, Gaebler C, et al. Anti-
2 SARS-CoV-2 receptor-binding domain antibody evolution after mRNA vaccination. *Nature*.
3 2021;600(7889):517-22.

4 45. Kim W, Zhou JQ, Horvath SC, Schmitz AJ, Sturtz AJ, Lei T, et al. Germinal centre-
5 driven maturation of B cell response to mRNA vaccination. *Nature*. 2022;604(7904):141-5.

6 46. Aikawa NE, Kupa LVK, Medeiros-Ribeiro AC, Saad CGS, Yuki EFN, Pasoto SG, et al.
7 Increment of immunogenicity after third dose of a homologous inactivated SARS-CoV-2
8 vaccine in a large population of patients with autoimmune rheumatic diseases. *Ann Rheum
9 Dis*. 2022;81(7):1036-43.

10 47. Bajwa HM, Novak F, Nilsson AC, Nielsen C, Holm DK, Ostergaard K, et al. Persistently
11 reduced humoral and sustained cellular immune response from first to third SARS-CoV-2
12 mRNA vaccination in anti-CD20-treated multiple sclerosis patients. *Mult Scler Relat Disord*.
13 2022;60:103729.

14 48. Herishanu Y, Rahav G, Levi S, Braester A, Itchaki G, Bairey O, et al. Efficacy of a third
15 BNT162b2 mRNA COVID-19 vaccine dose in patients with CLL who failed standard 2-dose
16 vaccination. *Blood*. 2022;139(5):678-85.

17 49. Funakoshi Y, Yakushijin K, Ohji G, Hojo W, Sakai H, Watanabe M, et al. Promising
18 Efficacy of a Third Dose of mRNA SARS-CoV-2 Vaccination in Patients Treated with Anti-
19 CD20 Antibody Who Failed 2-Dose Vaccination. *Vaccines (Basel)*. 2022;10(6).

20 50. van der Togt CJT, Ten Cate DF, van den Bemt BJF, Rahamat-Langendoen J, den
21 Broeder N, den Broeder AA. Seroconversion after a third COVID-19 vaccine is affected by
22 rituximab dose but persistence is not in patients with rheumatoid arthritis. *Rheumatology
23 (Oxford)*. 2022.

24 51. Stefanski AL, Rincon-Arevalo H, Schrezenmeier E, Karberg K, Szelinski F, Ritter J, et al.
25 Persistent but atypical germinal center reaction among 3(rd) SARS-CoV-2 vaccination after
26 rituximab exposure. *Front Immunol*. 2022;13:943476.

27 52. Akkaya M, Kwak K, Pierce SK. B cell memory: building two walls of protection against
28 pathogens. *Nat Rev Immunol*. 2020;20(4):229-38.

29 53. Purtha WE, Tedder TF, Johnson S, Bhattacharya D, Diamond MS. Memory B cells, but
30 not long-lived plasma cells, possess antigen specificities for viral escape mutants. *J Exp Med*.
31 2011;208(13):2599-606.

32 54. Goel RR, Painter MM, Lundgreen KA, Apostolidis SA, Baxter AE, Giles JR, et al.
33 Efficient recall of Omicron-reactive B cell memory after a third dose of SARS-CoV-2 mRNA
34 vaccine. *Cell*. 2022;185(11):1875-87 e8.

35 55. Muecksch F, Wang Z, Cho A, Gaebler C, Ben Tanfous T, DaSilva J, et al. Increased
36 memory B cell potency and breadth after a SARS-CoV-2 mRNA boost. *Nature*.
37 2022;607(7917):128-34.

38 56. Leandro MJ, Cambridge G, Ehrenstein MR, Edwards JC. Reconstitution of peripheral
39 blood B cells after depletion with rituximab in patients with rheumatoid arthritis. *Arthritis
40 Rheum*. 2006;54(2):613-20.

41 57. Anolik JH, Barnard J, Owen T, Zheng B, Kemshetti S, Looney RJ, et al. Delayed
42 memory B cell recovery in peripheral blood and lymphoid tissue in systemic lupus
43 erythematosus after B cell depletion therapy. *Arthritis Rheum*. 2007;56(9):3044-56.

44 58. Colucci M, Carsetti R, Cascioli S, Casiraghi F, Perna A, Rava L, et al. B Cell
45 Reconstitution after Rituximab Treatment in Idiopathic Nephrotic Syndrome. *J Am Soc
46 Nephrol*. 2016;27(6):1811-22.

1 59. Roll P, Dorner T, Tony HP. Anti-CD20 therapy in patients with rheumatoid arthritis:
2 predictors of response and B cell subset regeneration after repeated treatment. *Arthritis*
3 *Rheum.* 2008;58(6):1566-75.

4 60. Muhammad K, Roll P, Einsele H, Dorner T, Tony HP. Delayed acquisition of somatic
5 hypermutations in repopulated IgD+CD27+ memory B cell receptors after rituximab
6 treatment. *Arthritis Rheum.* 2009;60(8):2284-93.

7 61. Stefanski AL, Rincon-Arevalo H, Schrezenmeier E, Karberg K, Szelinski F, Ritter J, et al.
8 B Cell Numbers Predict Humoral and Cellular Response Upon SARS-CoV-2 Vaccination
9 Among Patients Treated With Rituximab. *Arthritis Rheumatol.* 2022;74(6):934-47.

10 62. Stefanski AL, Rincon-Arevalo H, Schrezenmeier E, Karberg K, Szelinski F, Ritter J, et al.
11 B Cell Characteristics at Baseline Predict Vaccination Response in RTX Treated Patients.
12 *Front Immunol.* 2022;13:822885.

13 63. Bitoun S, Henry J, Desjardins D, Vauloup-Fellous C, Dib N, Belkhir R, et al. Rituximab
14 Impairs B Cell Response But Not T Cell Response to COVID-19 Vaccine in Autoimmune
15 Diseases. *Arthritis Rheumatol.* 2022;74(6):927-33.

16 64. Jinich S, Schultz K, Jannat-Khah D, Spiera R. B Cell Reconstitution Is Strongly
17 Associated With COVID-19 Vaccine Responsiveness in Rheumatic Disease Patients Who
18 Received Treatment With Rituximab. *Arthritis Rheumatol.* 2022;74(5):776-82.

19

20

1 **Figure legends**

2 **Figure 1. Serological responses to Wild type SARS-CoV-2 antigens in Rituximab**

3 **treated patients after repeated vaccination.**

4 SARS-CoV-2 antibody profiles as determined using Luminex. The y-axis depicts mean
5 fluorescence intensity (MFI) levels. Sera were assessed at approximately one month after 1st
6 (1A, squares), 2nd (2A, circles), and 3rd (3A, diamonds) vaccine dose against Spike (A), RBD
7 (B) and Nucleocapsid (C) antigens. Symbols represent the MFI values for one sample,
8 whereas dotted lines connect samples from the same patient taken at different timepoints.
9 Unfilled symbols represent samples (number) where Luminex MFI data was unavailable.

10 **Figure 2. Serum neutralisation capacity and microfluidic antibody affinity profiling**

11 **against Wild type and Omicron variants in Rituximab treated patient cohort.**

12 Sera from Rituximab treated vasculitis patients were assessed at one month after 2nd (2A,
13 circles, n=14) and 3rd (3A, diamonds, n=14) vaccine doses for their neutralising capacity
14 (ND₅₀: 50% neutralising dose titre) against both Wild type (**A**) and Omicron (**D**) variants. All
15 sera were quantified using microfluidic antibody affinity profiling (MAAP) to measure the
16 affinity (K_D, M) and concentration ([Ab], M) of antibody binding sites that specifically bind
17 either the Wild Type (**B-C**) or Omicron (**E-F**) SARS-CoV-2 Spike RBD domains. There
18 were no significant differences between time points for any of the comparisons using either
19 paired (Wilcoxon paired signed ranked test) or unpaired (Mann-Whitney) statistical
20 assessments (p-values from Man-Whitney tests are shown). Dotted lines connect samples
21 taken from the same patient at different timepoints. Grey regions represent the lower limit of
22 the neutralisation assay. Unfilled symbols represent the samples (number) where MAAP data
23 was unobtainable due to non-binding or unquantifiable binding.

1 **Figure 3. SARS-CoV-2 antibody profiling in Rituximab treated patients showed**
2 **reduced neutralising capacity against the Omicron compared to Wild type (WT)**
3 **variants driven by weaker antibody affinity to the Omicron Spike RBD.**
4 Neutralising capacity (ND₅₀) of serum from Rituximab treated vasculitis patients against the
5 Omicron variant (red symbols) compared to the WT variant (blue symbols) at one month
6 after the 2nd vaccine dose (**A**; 2A, circles, p=0.0156), 3rd vaccine dose (**B**; 3A, diamonds,
7 p=0.0312), or when data from both timepoints were combined (**C**; 2A+3A, triangles,
8 p=0.0002). Microfluidic antibody affinity profiling to measure antibody affinity (K_D, M) and
9 binding site concentration ([Ab], M) demonstrated no difference in the concentration of
10 antibodies recognising the WT and Omicron RBD variants (**D**, p=0.2412), but weaker
11 antibody affinity against the Omicron strain (**E**, p=0.0004). Dotted lines connect identical
12 samples assessed against different variants. Unfilled symbols represent the samples (number)
13 where MAAP data was unobtainable due to insufficient or unquantifiable binding. P-values
14 presented are two-tailed from the Wilcoxon paired signed-ranks test.

15 **Figure 4. Anti-SARS-CoV-2 antibody profiling in healthy individuals versus Rituximab**
16 **treated patients.**

17 Serum neutralising titres (ND₅₀) in healthcare workers (HCW) versus Rituximab (RTX)
18 treated vasculitis patients one month after the third exposure to SARS-CoV-2 antigen (3A)
19 assessed against Wild type (**A**; p=0.0004) and Omicron strains (**B**; p=0.003). Comparison of
20 quantifiable antibodies to Wild type SARS-CoV-2 using microfluidic affinity profiling
21 (MAAP) showed similar affinity (**C**; p=0.5825), but lower abundance in Rituximab treated
22 patients (**E**; p=0.0018). In contrast, the abundance of antibodies against the RBD Omicron
23 variant was comparable between the cohorts (**F**; p=0.3169), however these antibodies were of
24 higher affinity in the HCW cohort (**D**; p=0.0002). In **A-B**, the grey region represents the
25 lower limit of detection for the neutralisation assay. Box blots represent the median, range

1 and interquartile range for each dataset. Unfilled symbols in **C-F** represent samples (number)
2 where MAAP data was unobtainable due to insufficient or unquantifiable binding. Statistical
3 analysis was carried out for each plot via Mann Whitney Test and presented p-values are two-
4 tailed.

5 **Figure 5. Microfluidic antibody affinity profiling (MAAP) of the evolution of the**
6 **antibody response after infection with Wild type SARS-CoV-2.**

7 Anti-SARS-CoV-2 Wild type Spike RBD antibody affinity (K_D , M) and binding site
8 concentration ([Ab], M) in sera from convalescent patients at one- (1A) and three-months
9 (1B) post-infection were assessed using MAAP. Panel **A** shows that the concentration of
10 antibodies decreased over time (**A**; $p=0.0034$), but their affinity against RBD increased (**B**;
11 $p=0.0244$), resulting in an overall decrease in serum neutralisation capacity (**C**; $p=0.0296$).
12 Dotted lines connect samples taken from the same patient at the two timepoints. Unfilled
13 symbols in **A-B** represent samples (number) where MAAP data was unobtainable due to
14 insufficient or unquantifiable binding. Presented p-values are two-tailed from the Wilcoxon
15 paired signed rank test.

16 **Figure 6. Antibody profiling against Wild type SARS-CoV-2 in Convalescent versus**
17 **Rituximab treated patients.**

18 Comparison of serum neutralising titres (ND_{50}) in convalescent patients one month after Wild
19 type SARS-CoV-2 infection (Conv. 1A) versus in Rituximab treated patients at one month
20 following the second (RTX 2A) and third vaccine doses (RTX 3A) showed numerically
21 higher, but not statistically different titres in the two cohorts (**A**; Conv. 1A vs RTX 2A:
22 $p=0.2832$ and Conv. 1A vs RTX 3A: $p=0.5515$). Comparison of quantifiable antibodies to
23 Wild type SARS-CoV-2 using microfluidic affinity profiling (MAAP) showed similar
24 antibody affinity (**B**; Conv. 1A vs RTX 2A: $p=0.2236$ and Conv. 1A vs RTX 3A: $p=0.3002$)
25 and antibody concentration (**C**; Conv. 1A vs RTX 2A: $p>0.9999$ and Conv. 1A vs RTX 3A:

1 p=0.6399). Box blots represent the median, range and interquartile range for each dataset.
2 Grey shading in A represents the lower assay limit. Unfilled symbols in B-C represent
3 samples (number) where MAAP data was unobtainable due to insufficient or unquantifiable
4 binding. Statistical analysis was carried out using Kruskal-Wallis ANOVA test (presented)
5 and Dunn's multiple comparisons and all p-values are two-tailed.

6 **Figure 7. Global analysis of antibody fingerprints to SARS-CoV-2 Wild type and**
7 **Omicron variants across all patient cohorts and correlation with clinically relevant**
8 **parameters.**

9 **Panel A. Antibody affinity and concentration across different patient cohorts and**
10 **variants.** The contour map summarises the equilibrium dissociation constant (K_D) vs the
11 concentration of antibody binding sites ([AB]) across three cohorts: Conv. 1A (convalescent
12 COVID-19 1-month post-infection, green), RTX 3A (Rituximab cohort 1-month after 3rd
13 vaccine dose, yellow), and HCW 3A (health care worker cohort 1-month after infection and 2
14 vaccinations, red); the colour gradient is proportional to the expected probability. The filling
15 colour of points indicates the variant. Wild type (WT) and Omicron points from the same
16 sample are linked by dashed lines. The x-axis depicts increased affinity i.e. lower K_D values
17 towards the right; higher concentrations of antibody binding sites are displayed, in increasing
18 order, on the y-axis.

19 **Panel B. Comparison of antibody affinity and concentration across sex and SARS-CoV-**
20 **2 variants.** The plots summarise the product of equilibrium dissociation constant (K_D) and
21 concentration of antibody binding sites ([AB]) in relation to sex and SARS-CoV-2 variants
22 (WT and Omicron) across three cohorts: Conv. 1A (convalescent COVID-19 1-month post-
23 infection, circles), RTX 3A (Rituximab cohort 1-month after 3rd vaccine, squares), and HCW
24 3A (health care worker cohort 1-month after infection and 2 vaccinations, triangles). On the
25 x-axis, the multiplicative classes on sex (male or female) and variant are represented. The y-

1 axis represents the product of K_D and $[AB]$ (no units). No significant differences in the
2 product of antibody affinity and concentration were noted between female and male
3 individuals for both Omicron ($p=0.0617$) and WT ($p=0.0539$); p -values are from Mann-
4 Whitney U test.

5 **Panel C. Comparison of antibody affinity and concentration according to patient age**
6 **and SARS-CoV-2 variant.** This scatter plot with a linear regression line depicts the
7 interaction between age (y-axis) and the product of the equilibrium dissociation constant (K_D)
8 and concentration of antibody binding sites ($[AB]$) (x-axis), across the variants (WT and
9 Omicron) and cohorts: Conv. 1A (convalescent COVID-19 1-month post-infection, circles),
10 RTX 3A (Rituximab cohort 1-month after 3rd vaccine, squares), and HCW 3A (health care
11 worker cohort 1-month after infection and 2 vaccinations, triangles). A linear model fit
12 (smooth line) and the Spearman rank correlation coefficient is depicted, indicating the
13 strength and direction of the correlation between age and $[AB] \times K_D$.

14 **Panel D. Relationship between COVID-19 disease severity and the product of antibody**
15 **affinity and binding site concentration ($\log(AB \times K_D)$ at 1-month post-infection in the**
16 **convalescent cohort.** Convalescent patients after more severe disease showed a trend
17 towards higher antibody responses ($[AB] \times K_D$) to WT SARS-CoV-2 one month after infection
18 compared to asymptomatic patients and those with mild disease (Kruskal-Wallis rank sum
19 test: $p=0.08$; pairwise comparisons with Benjamini-Hochberg multiple testing correction:
20 $p>0.05$ for all comparisons).

21 Disease severity was classified as follows: (A) asymptomatic; (B) mild symptoms not
22 requiring hospitalisation; (C) patients who presented to hospital but never required oxygen
23 supplementation; (D) patients who were admitted to hospital and whose maximal respiratory
24 support was supplemental oxygen; and (E) patients who at some point required assisted
25 ventilation.

1 **Figure 8. Multidimensional assessment of SARS-CoV-2 antibody profiles at the**
2 **individual patient level.**

3 **Panel A. Summary heatmap depicting key immunological and demographic metrics**
4 **across different cohorts and timepoints.** Each row corresponds to a single participant in the
5 study, grouped per cohort affiliation (Left hand side colour bar). Columns correspond to
6 several measurements, structured into four main categories: Luminex MFI, KD, [Ab], and
7 ND₅₀. Each of these categories contains measurements at three distinct time points which are
8 denoted by the top colour bar. Luminex MFI has a breakdown into N, S, and RBD. For KD,
9 [Ab], and ND₅₀, measurements are differentiated by the variant of the virus (WT or
10 Omicron). Colour intensity within the heatmap corresponds to the log-transformed value of
11 each measurement, with darker hues indicating higher values (except in KD as lower values
12 correspond to higher antibody affinity). Age, sex, and ethnicity of participants are also
13 visualised in the right-hand side columns.

14 **Panel B. Relationship between serum Wild type SARS-CoV-2 neutralisation titre**
15 **(logND₅₀) and antibody binding site concentration ([Ab}, M) across timepoints and**
16 **patient cohorts.** Data points from each patient cohort are represented by different shapes. A
17 linear model fit (smooth line) is shown and the Spearman correlation coefficient is depicted,
18 indicating the strength and direction of the correlation between [AB] and ND₅₀. The
19 Spearman correlation coefficients for data in each patient cohort are also shown.

20 **Panel C. Relationship between serum Wild type SARS-CoV-2 neutralisation titre**
21 **(logND₅₀) and Luminex anti-RBD MFI across patient cohorts.** Data points from each
22 patient cohort are represented by different colours. A linear model fit (smooth line) is shown
23 and the Spearman correlation coefficient is depicted, indicating the strength and direction of
24 the correlation between ND₅₀ and Luminex RBD MFI. The Spearman correlation coefficients
25 for data in each patient cohort are also shown.

(A)

Spike Protein

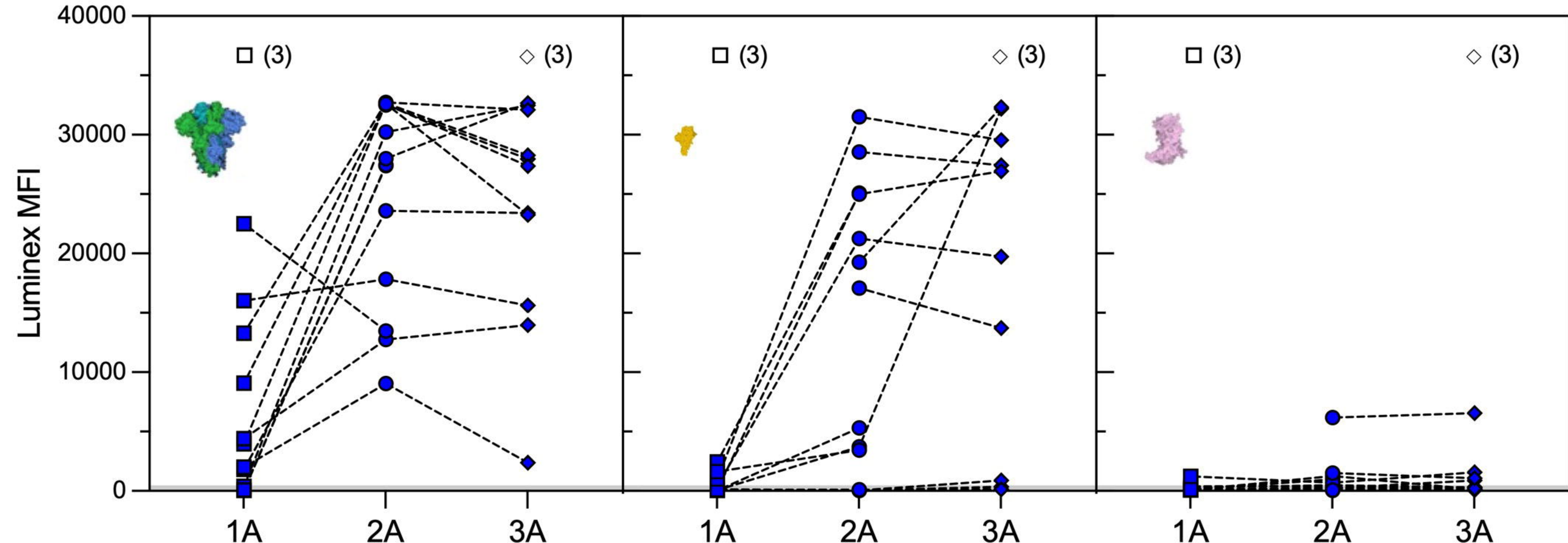
bioRxiv preprint doi: <https://doi.org/10.1101/2023.10.22.563481>; this version posted October 24, 2023. The copyright holder for this preprint (which was not certified by peer review) is the author/funder, who has granted bioRxiv a license to display the preprint in perpetuity. It is made available under aCC-BY-ND 4.0 International license.

(B)

Spike RBD Protein

(C)

Nucleocapsid Protein

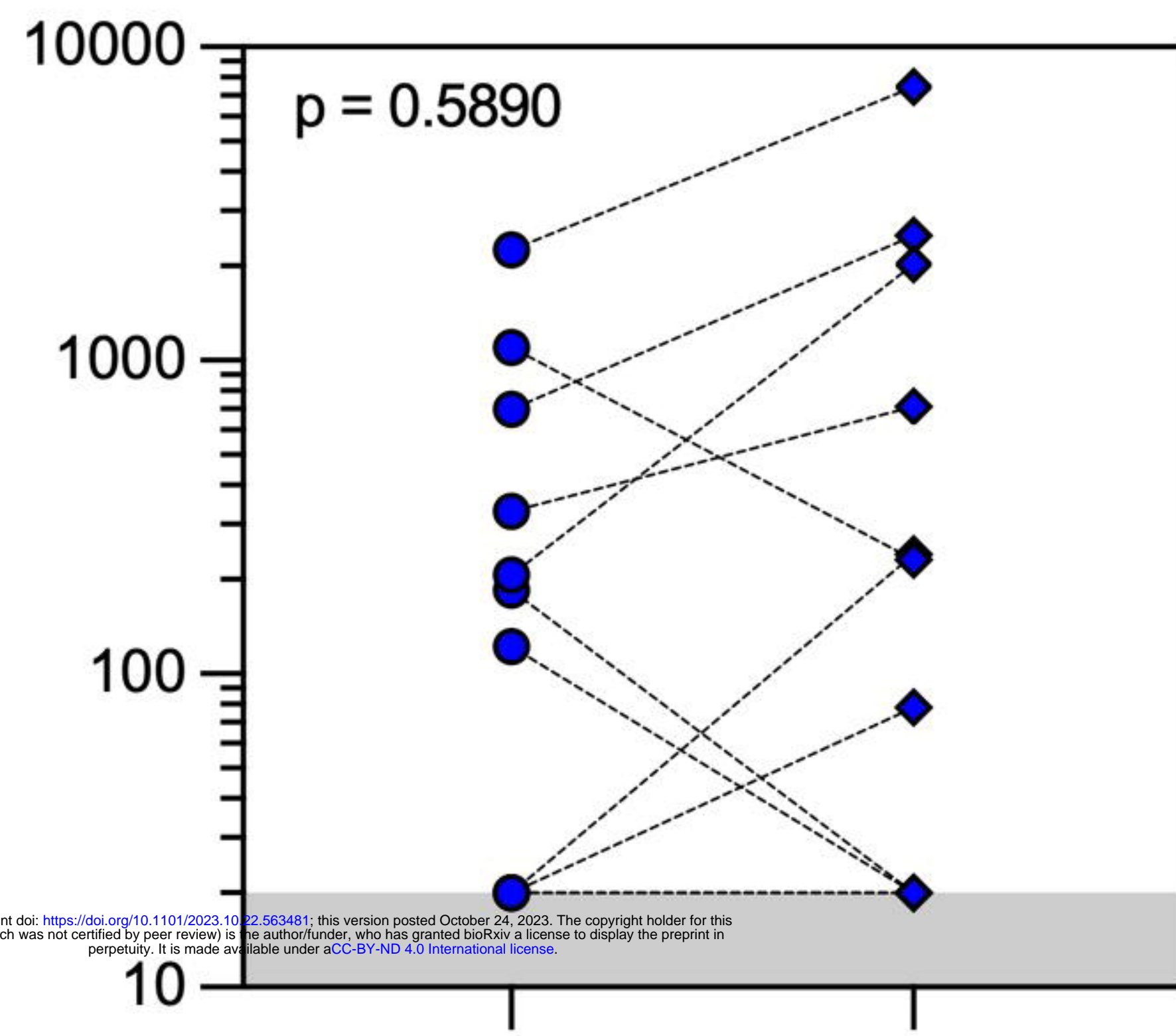


Neutralisation (ND₅₀)

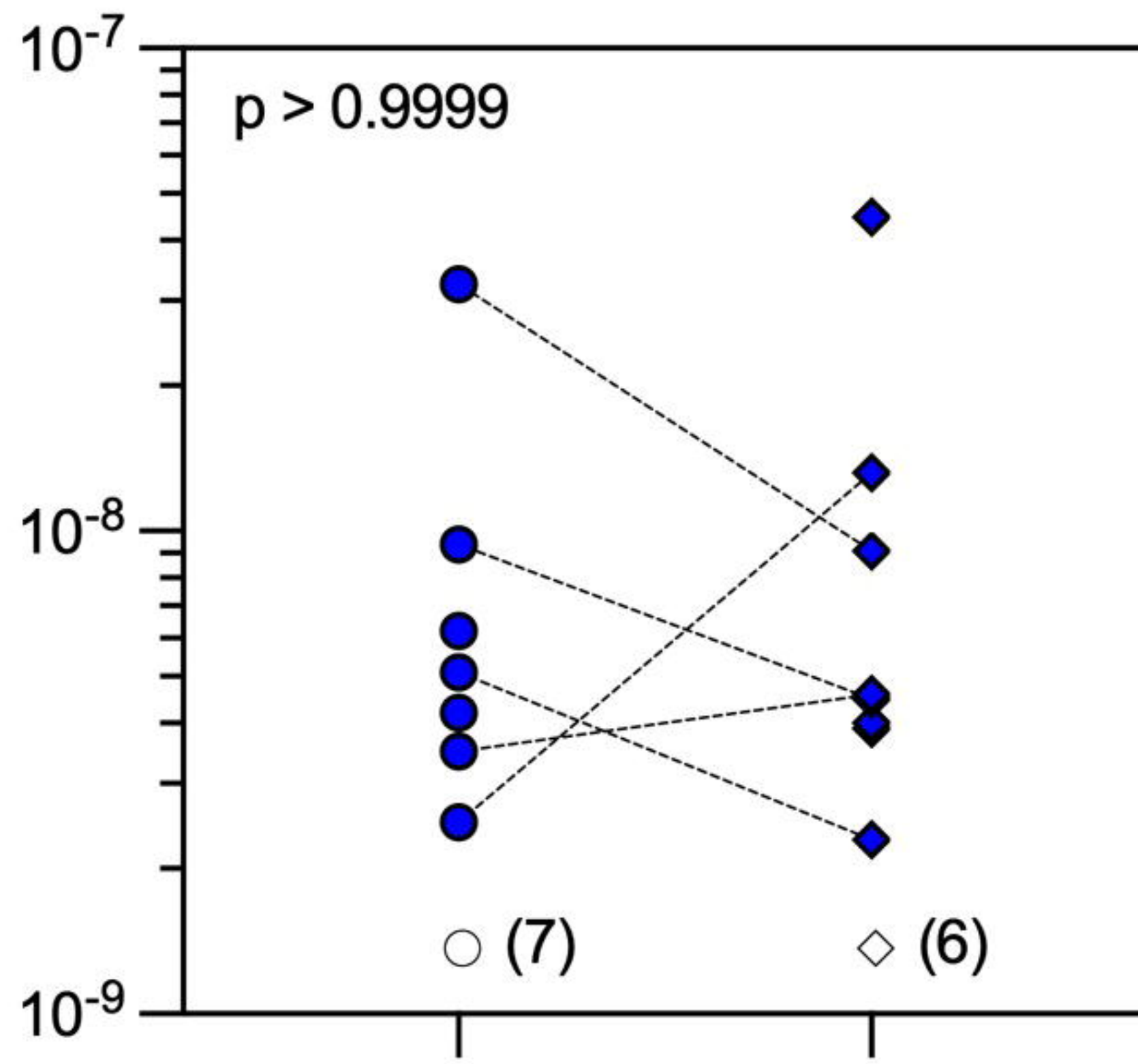
K_D (M)

[Ab] (M)

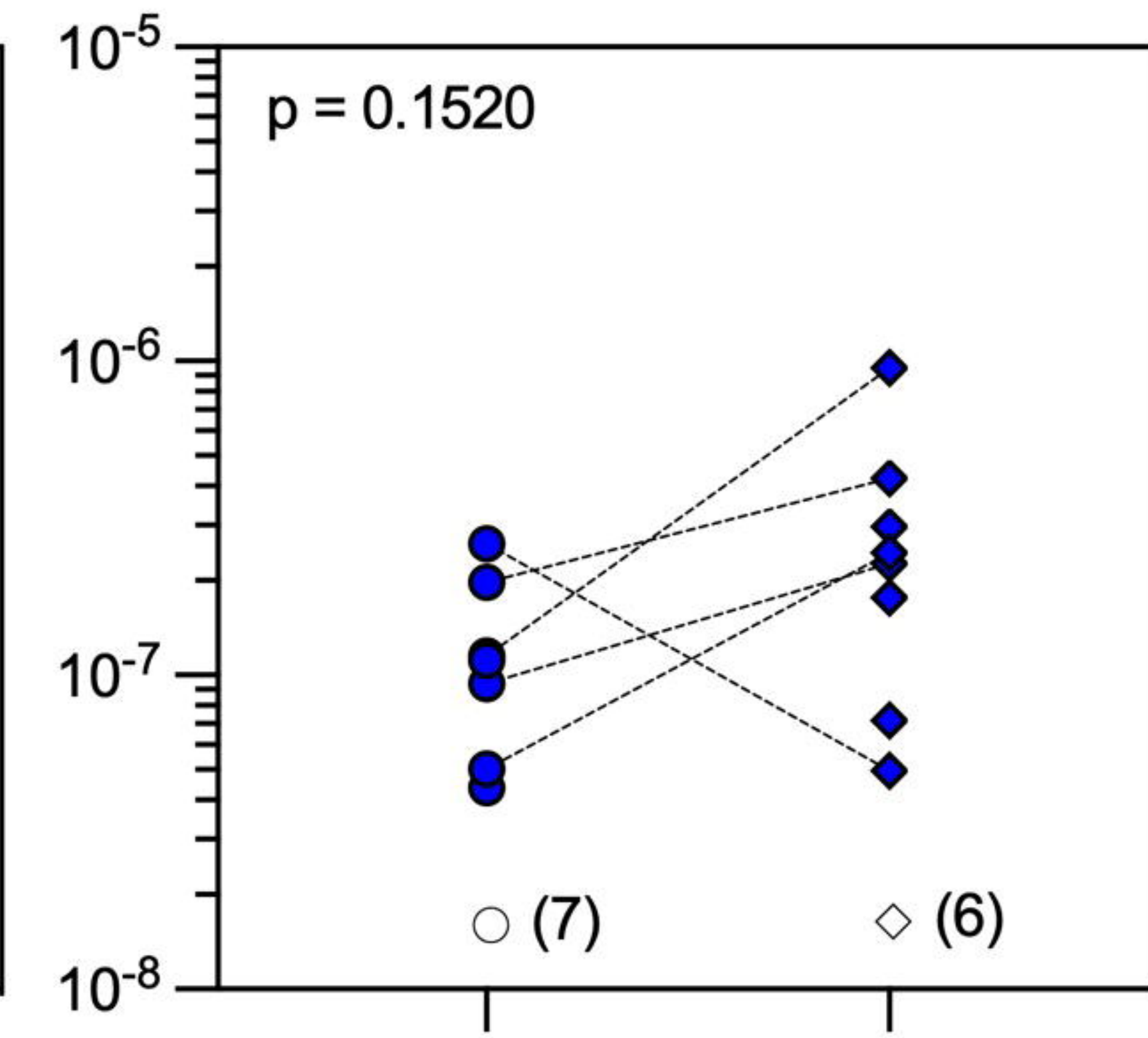
(A)



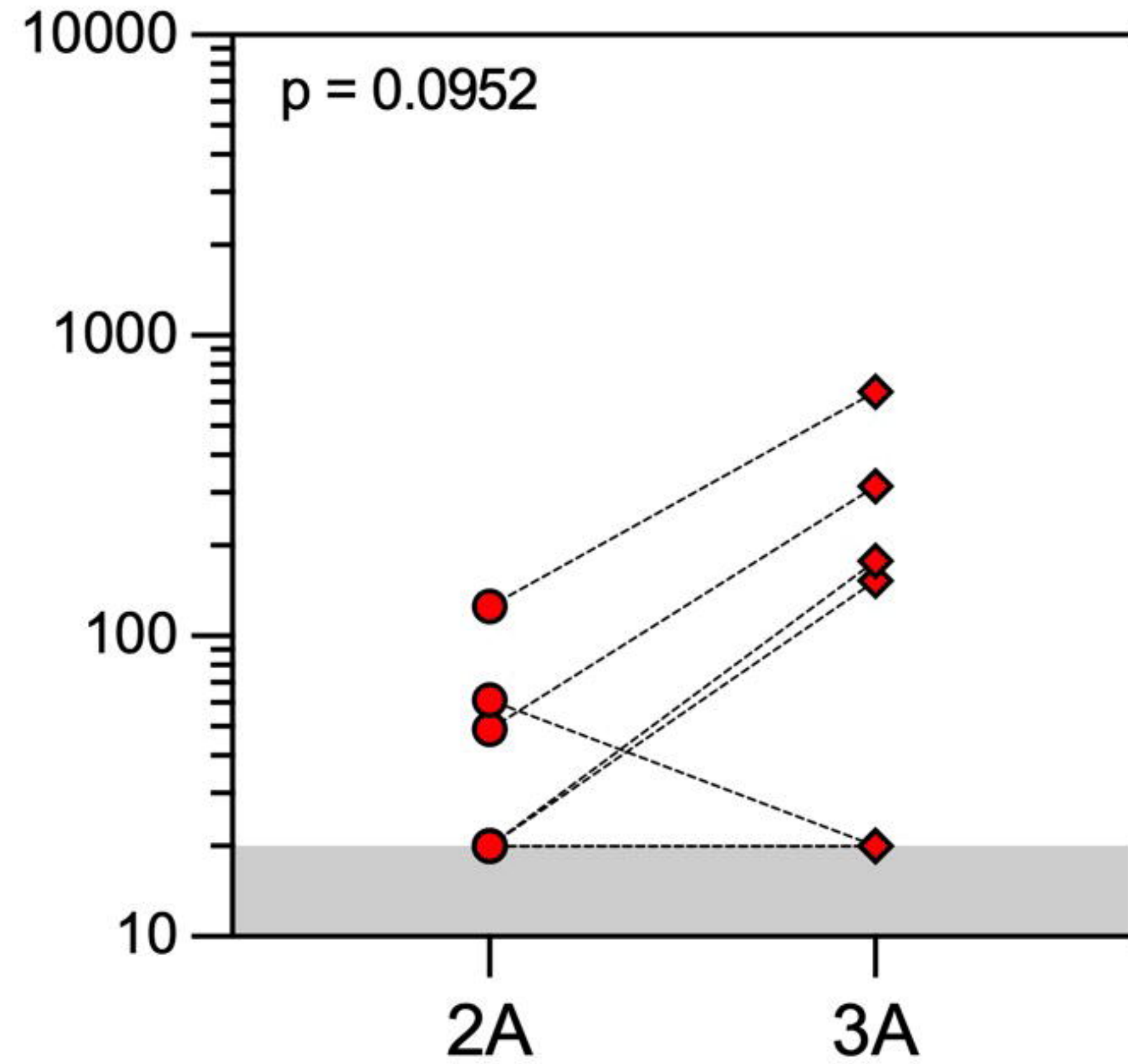
(B)



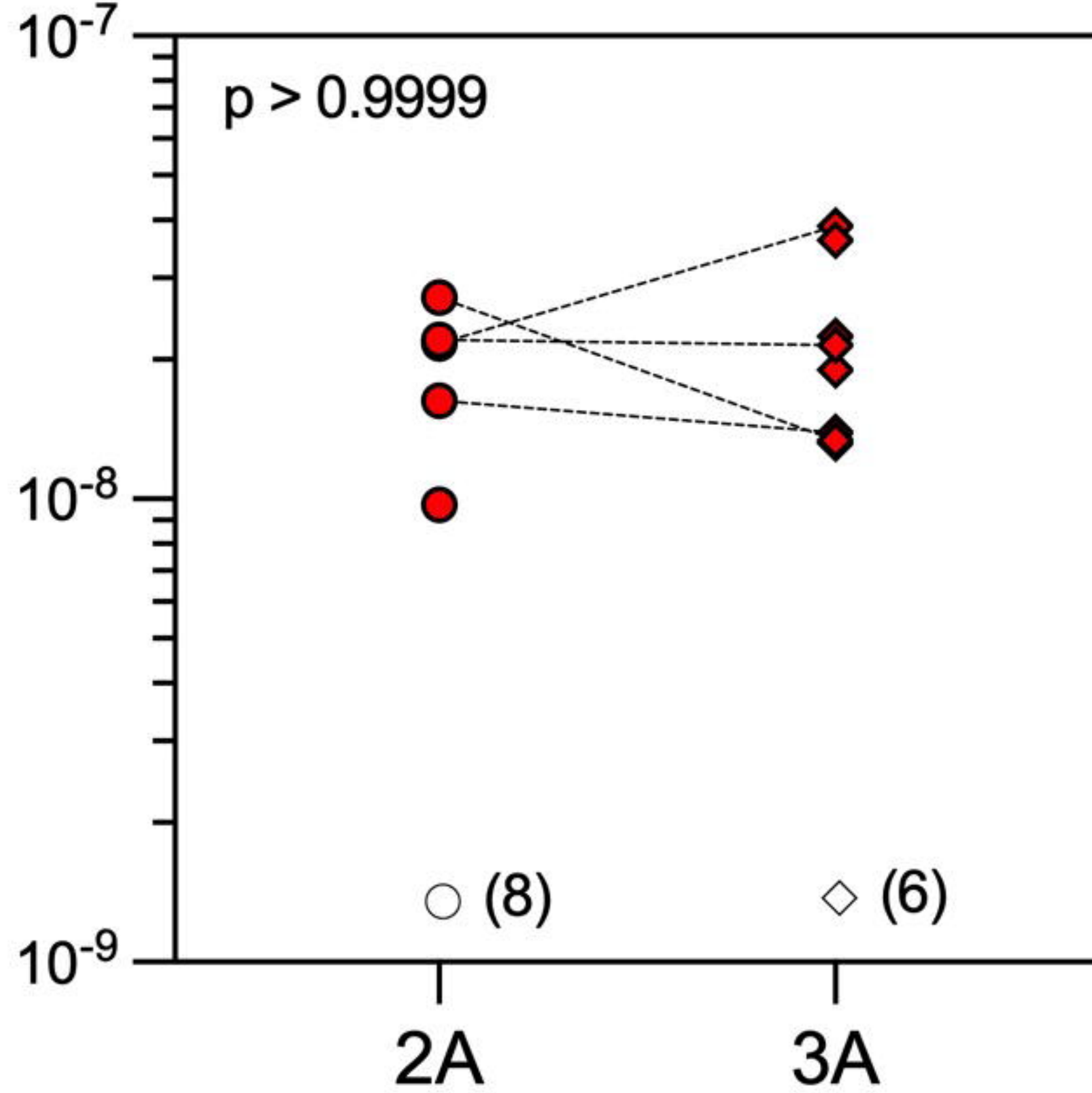
(C)



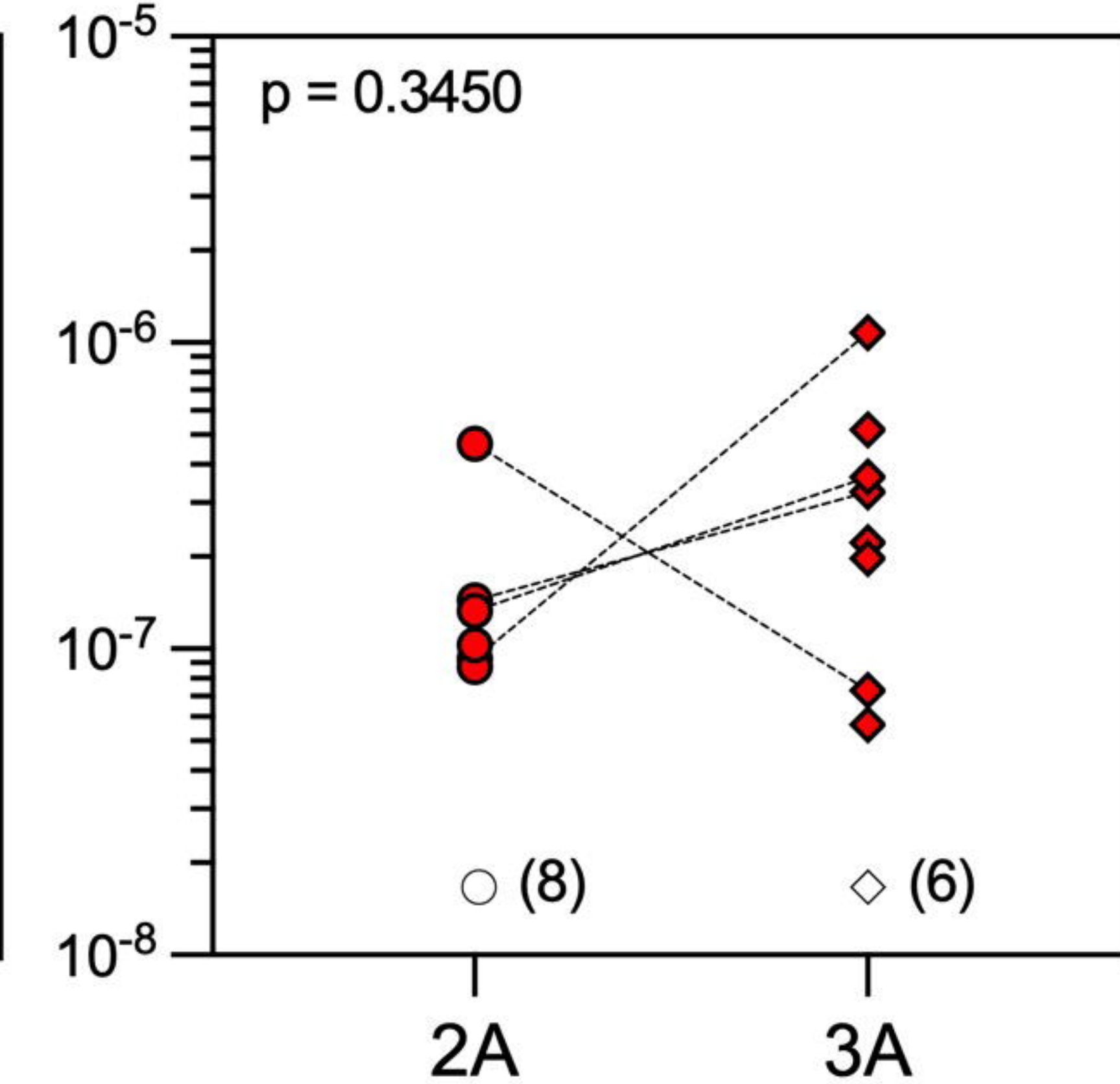
(D)



(E)



(F)

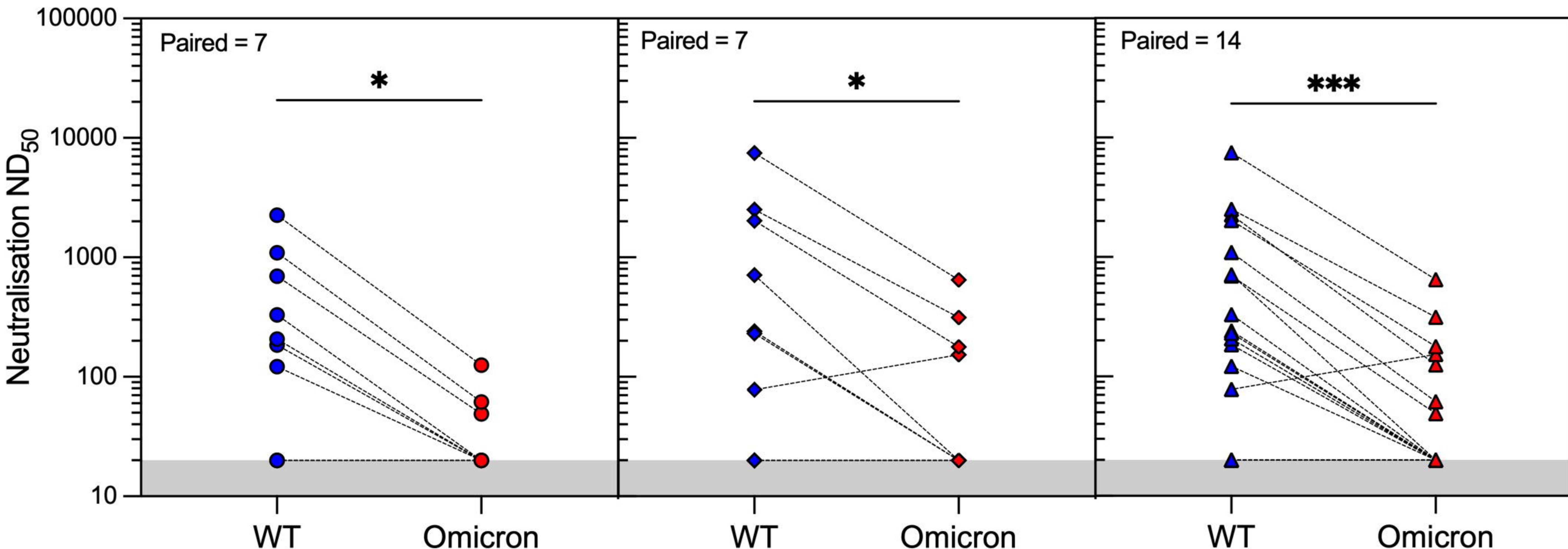


(A)**(B)****(C)**

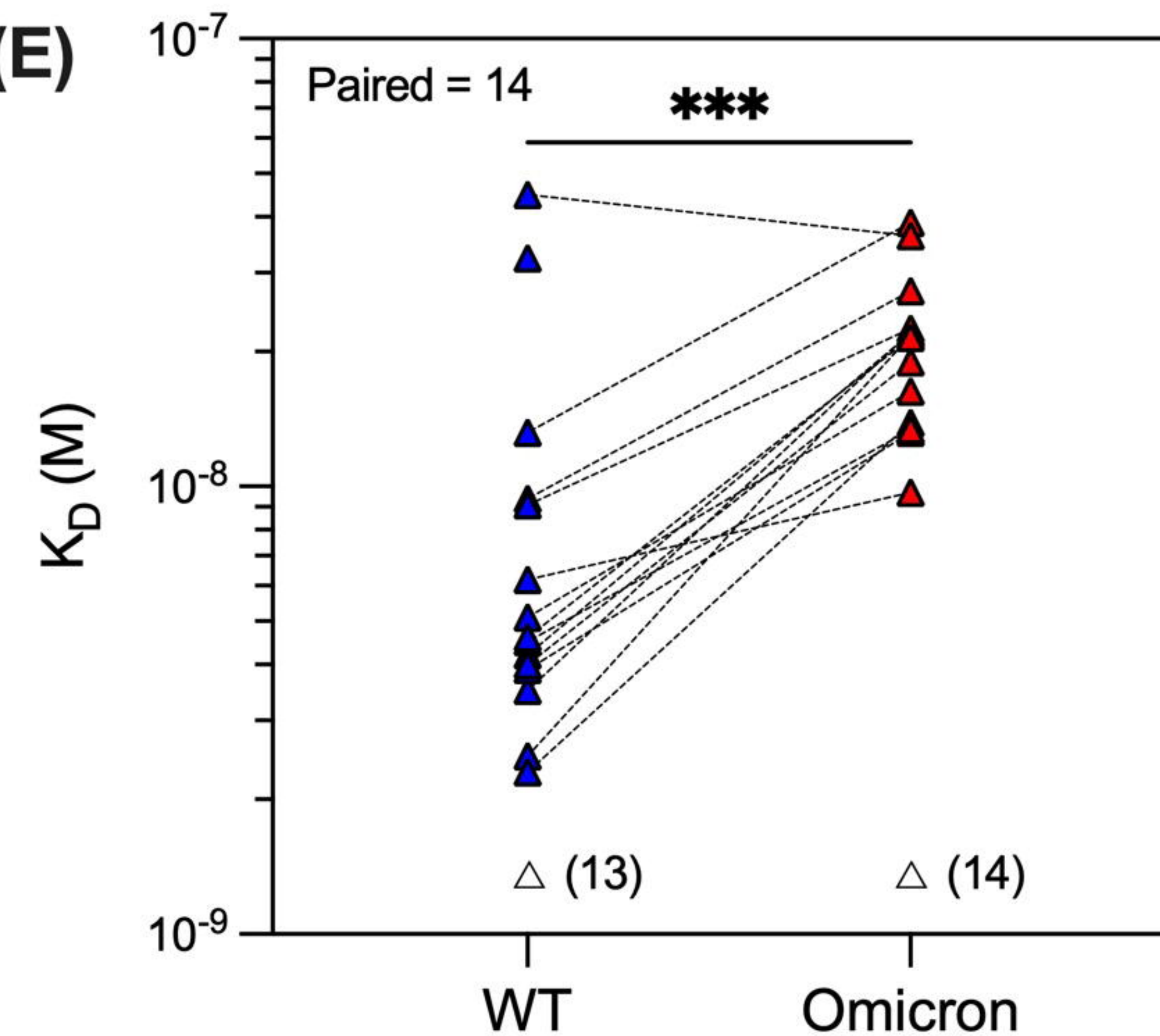
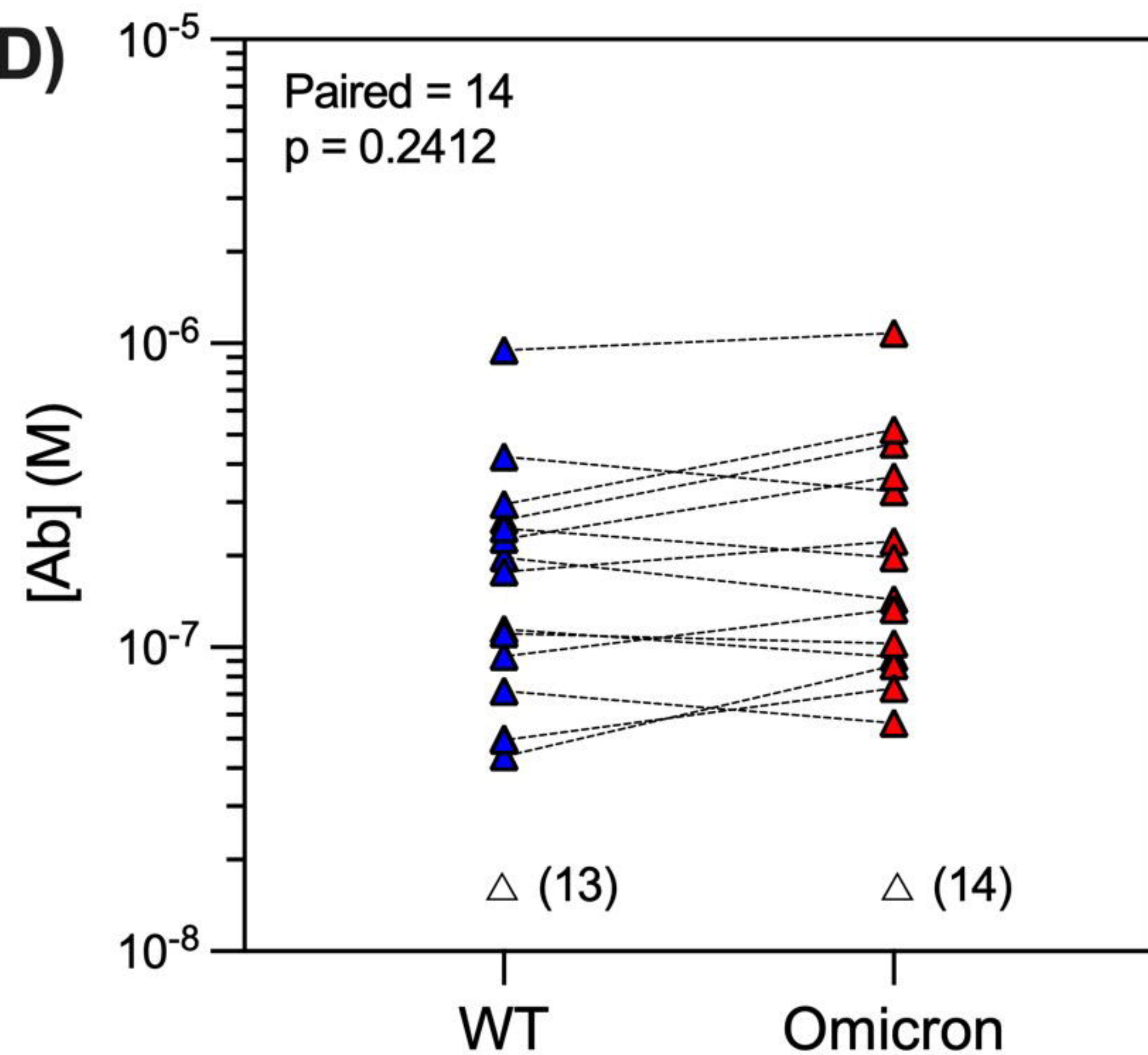
2A

3A

2A + 3A



bioRxiv preprint doi: <https://doi.org/10.1101/2023.10.22.563481>; this version posted October 24, 2023. The copyright holder for this preprint (which was not certified by peer review) is the author/funder, who has granted bioRxiv a license to display the preprint in perpetuity. It is made available under aCC-BY-ND 4.0 International license.

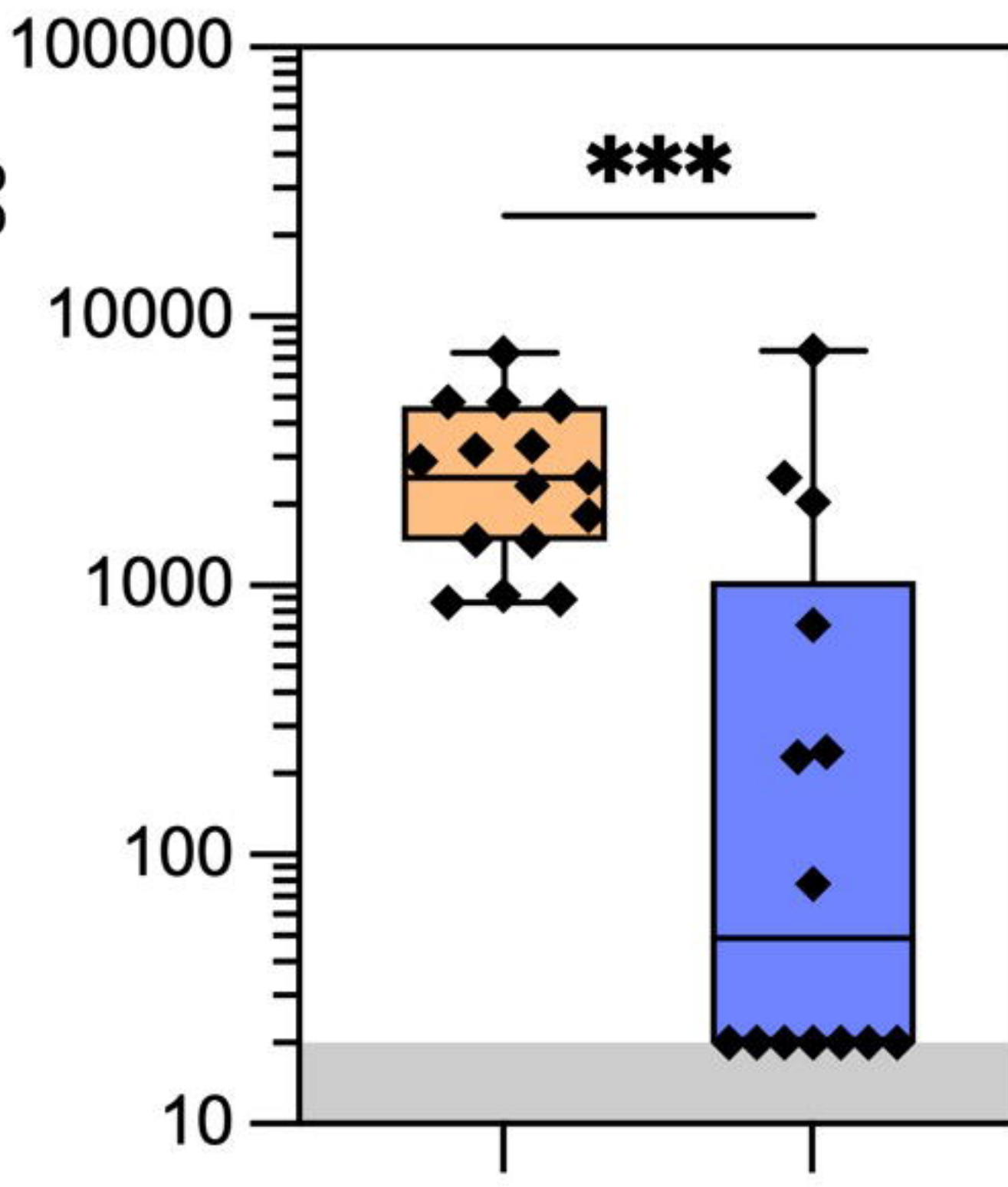
(D)**(E)**

WT

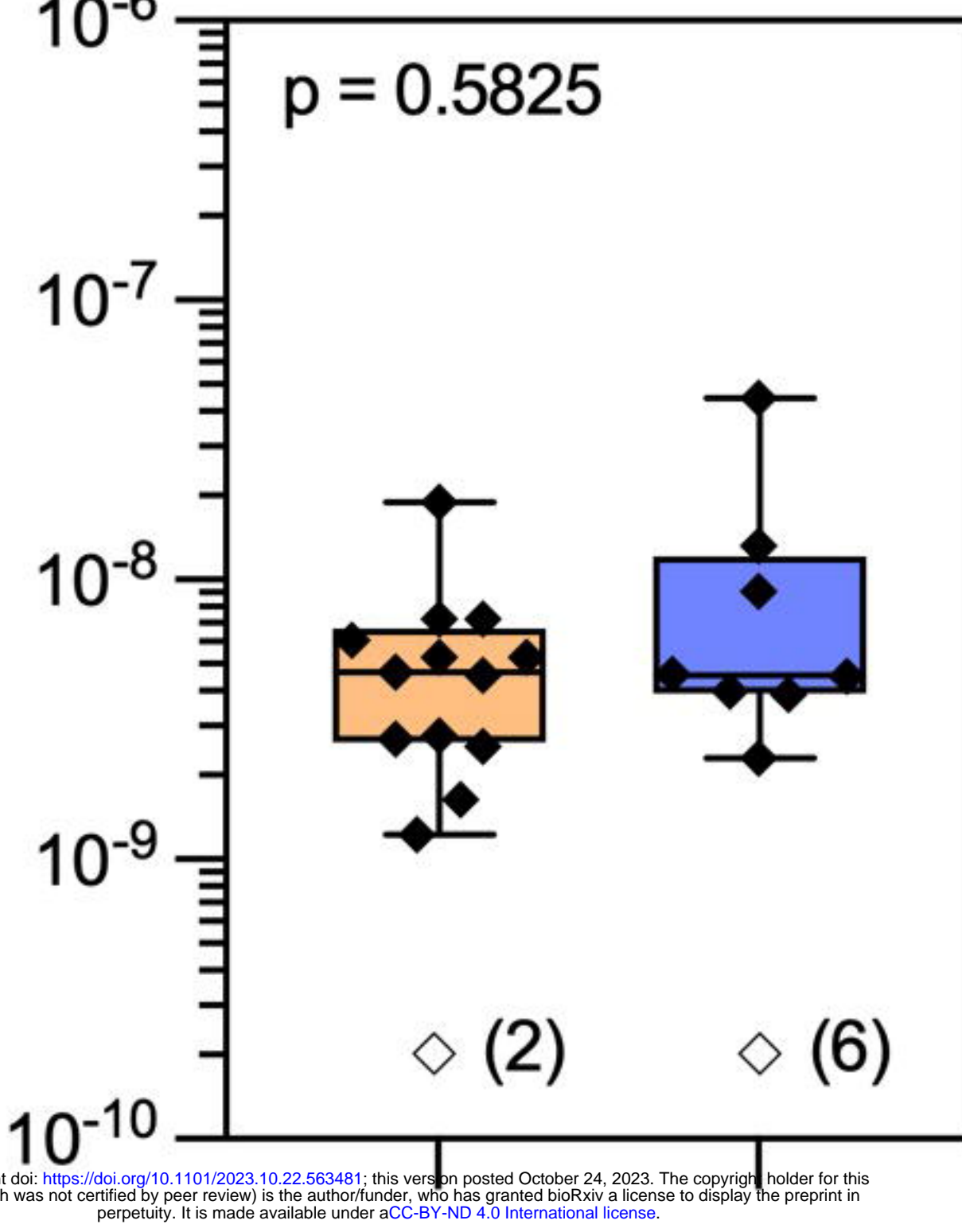
Omicron

(A)

(B)

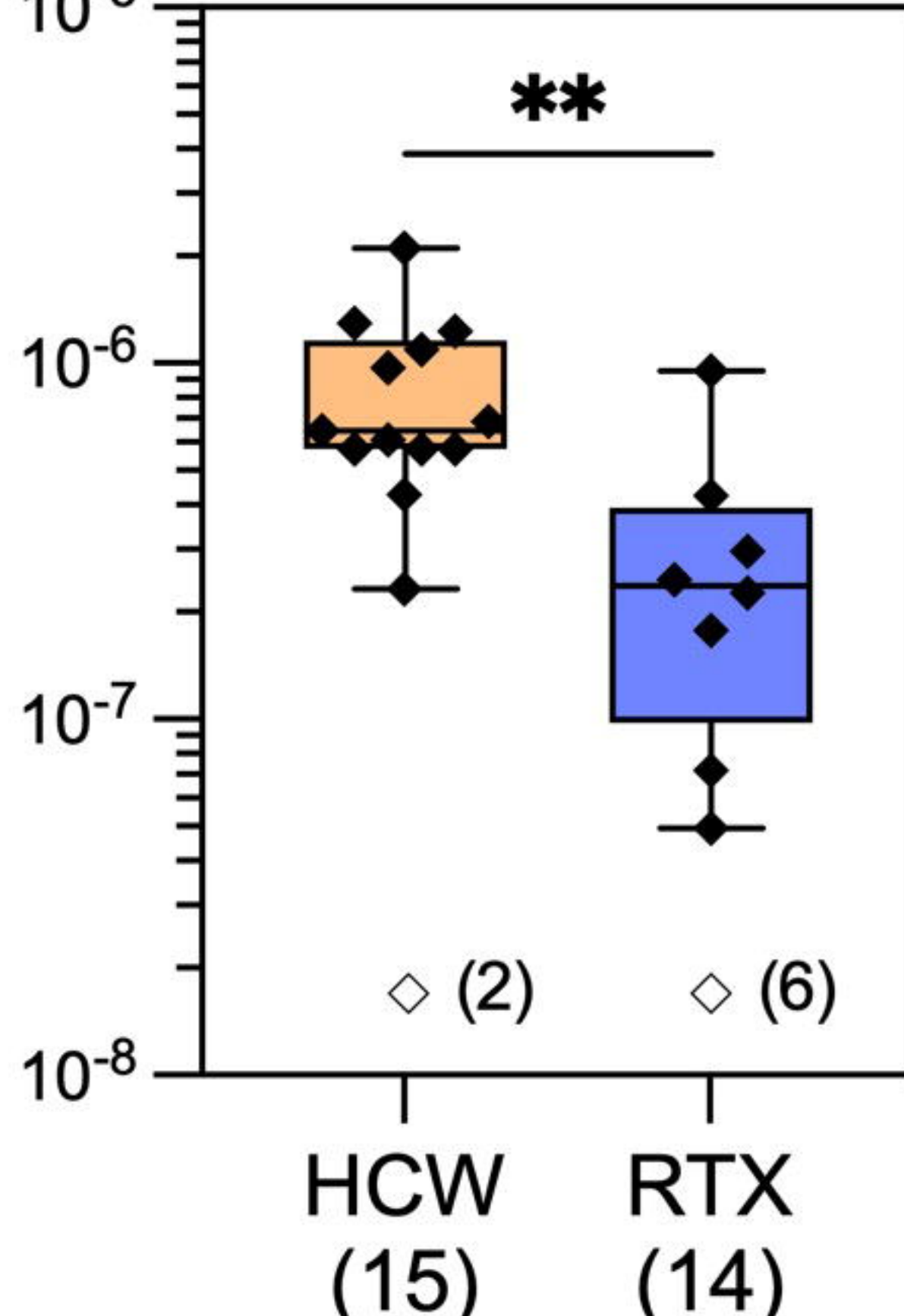
Neutralisation ND₅₀

(D)

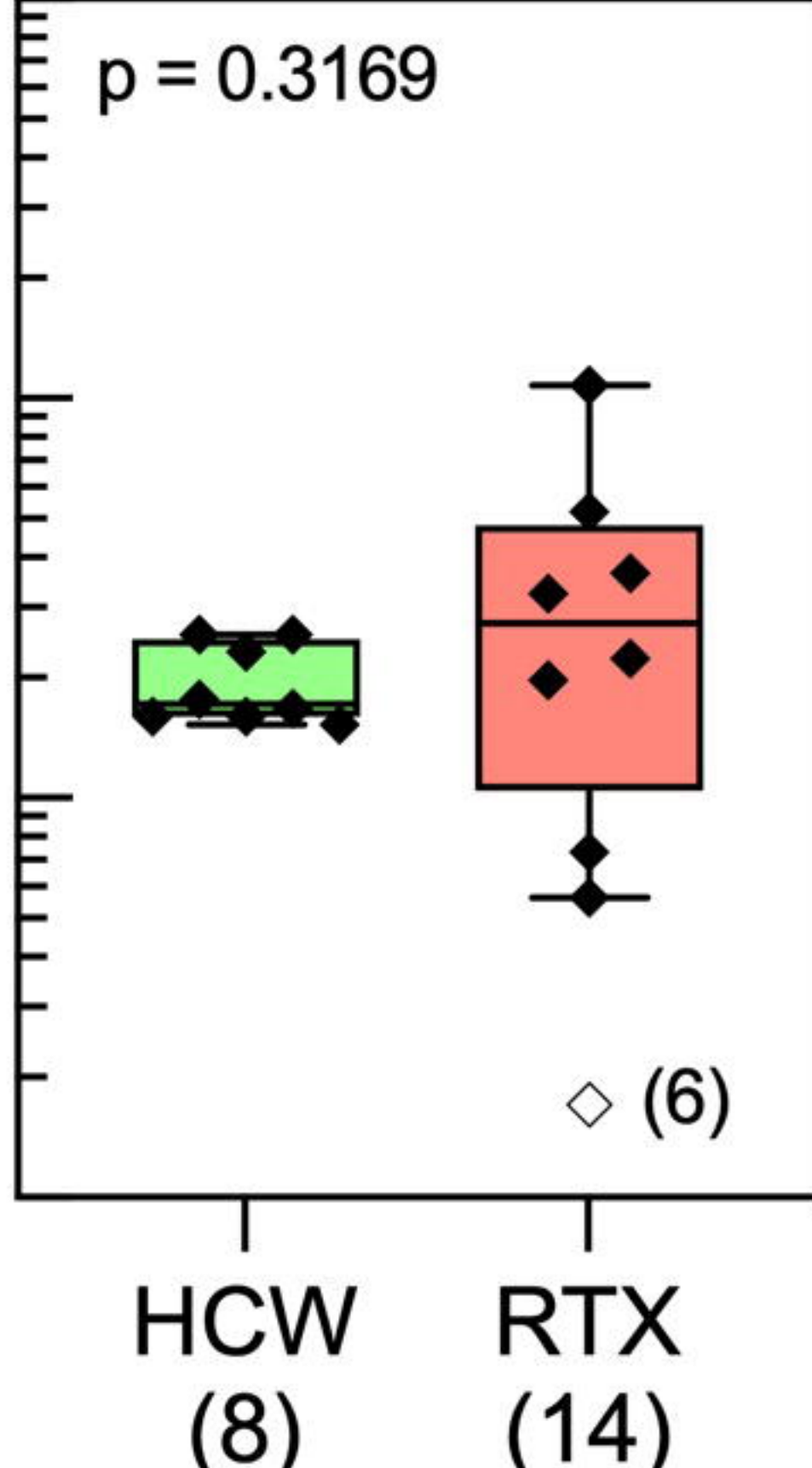


(E)

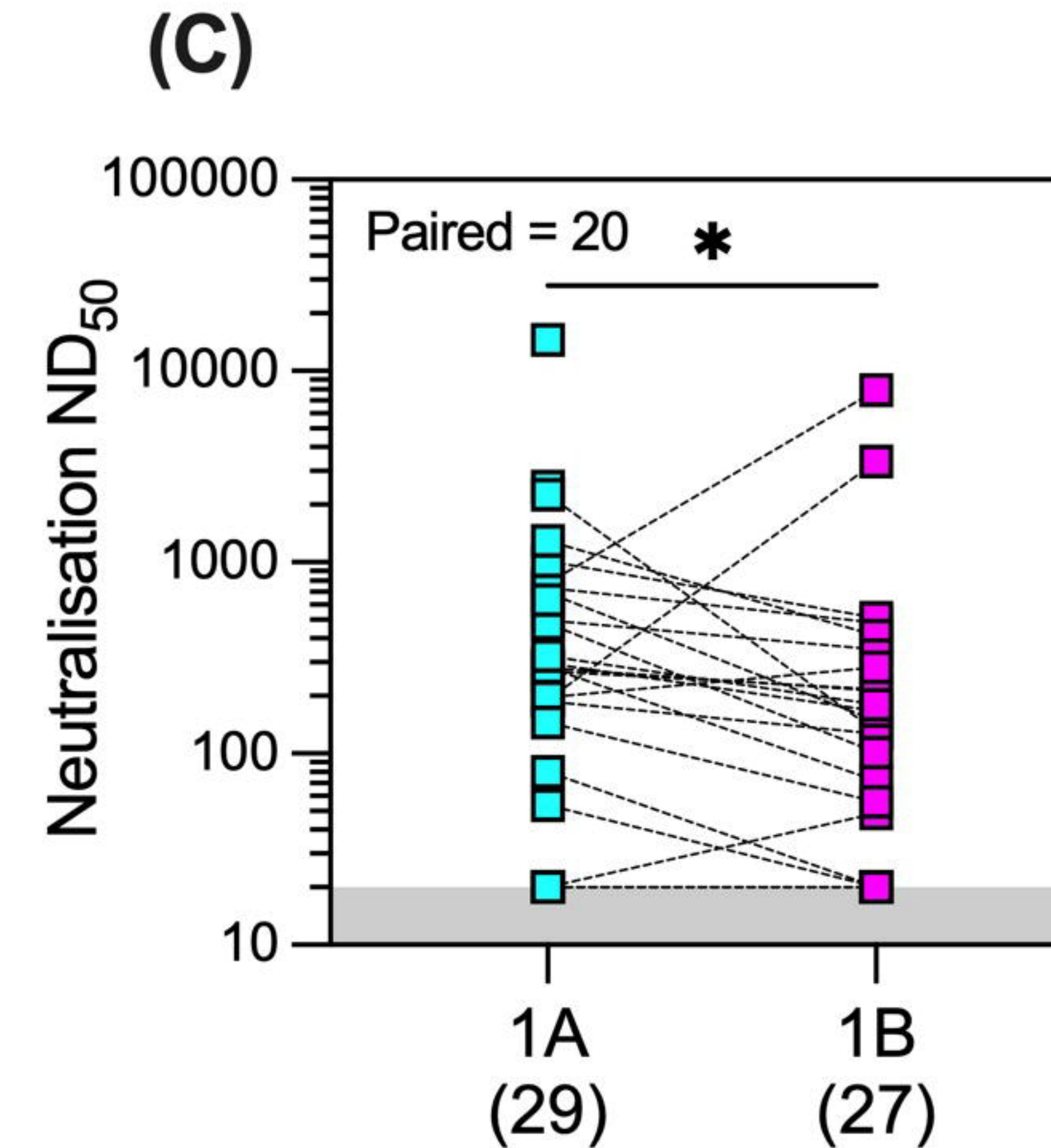
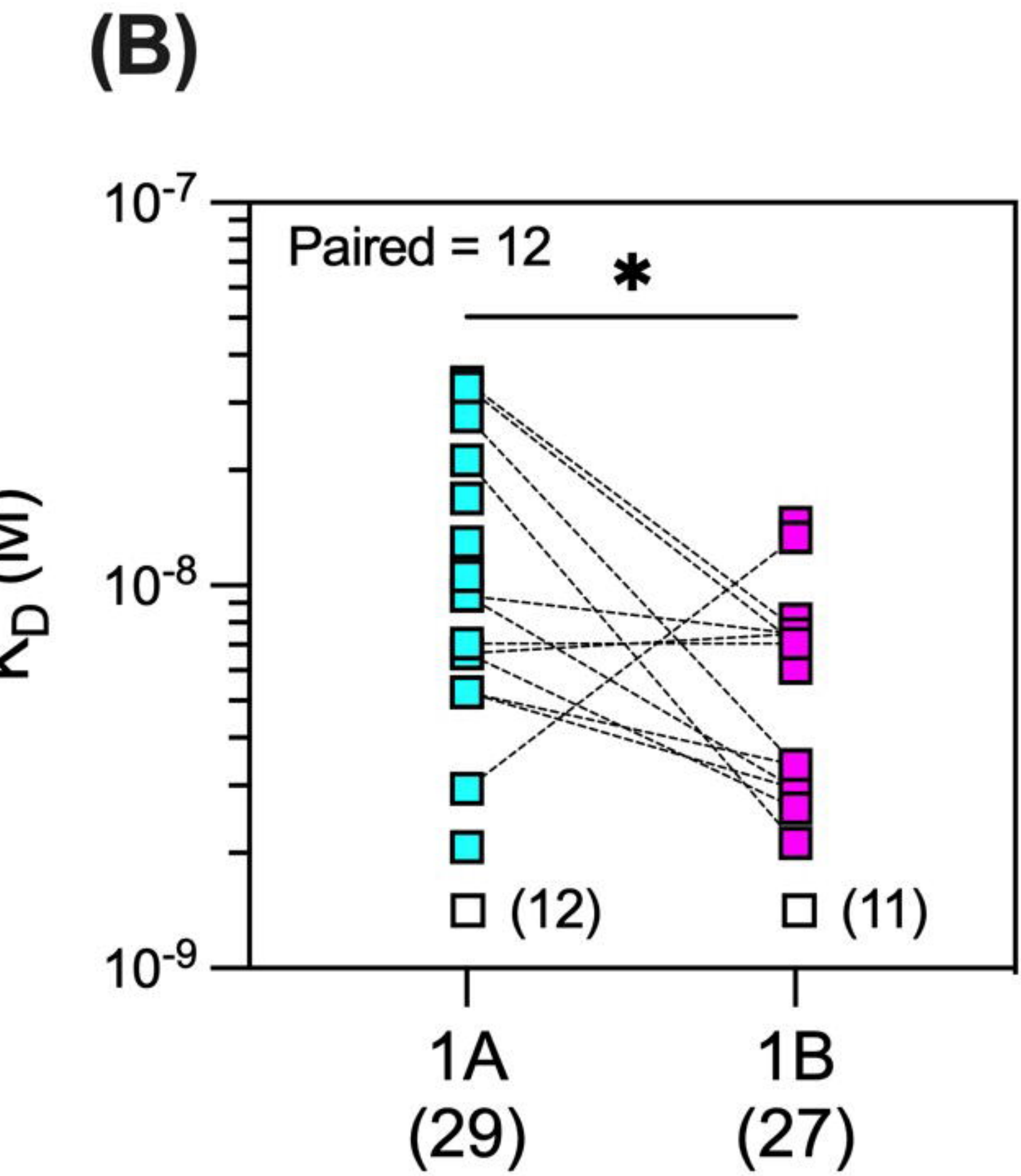
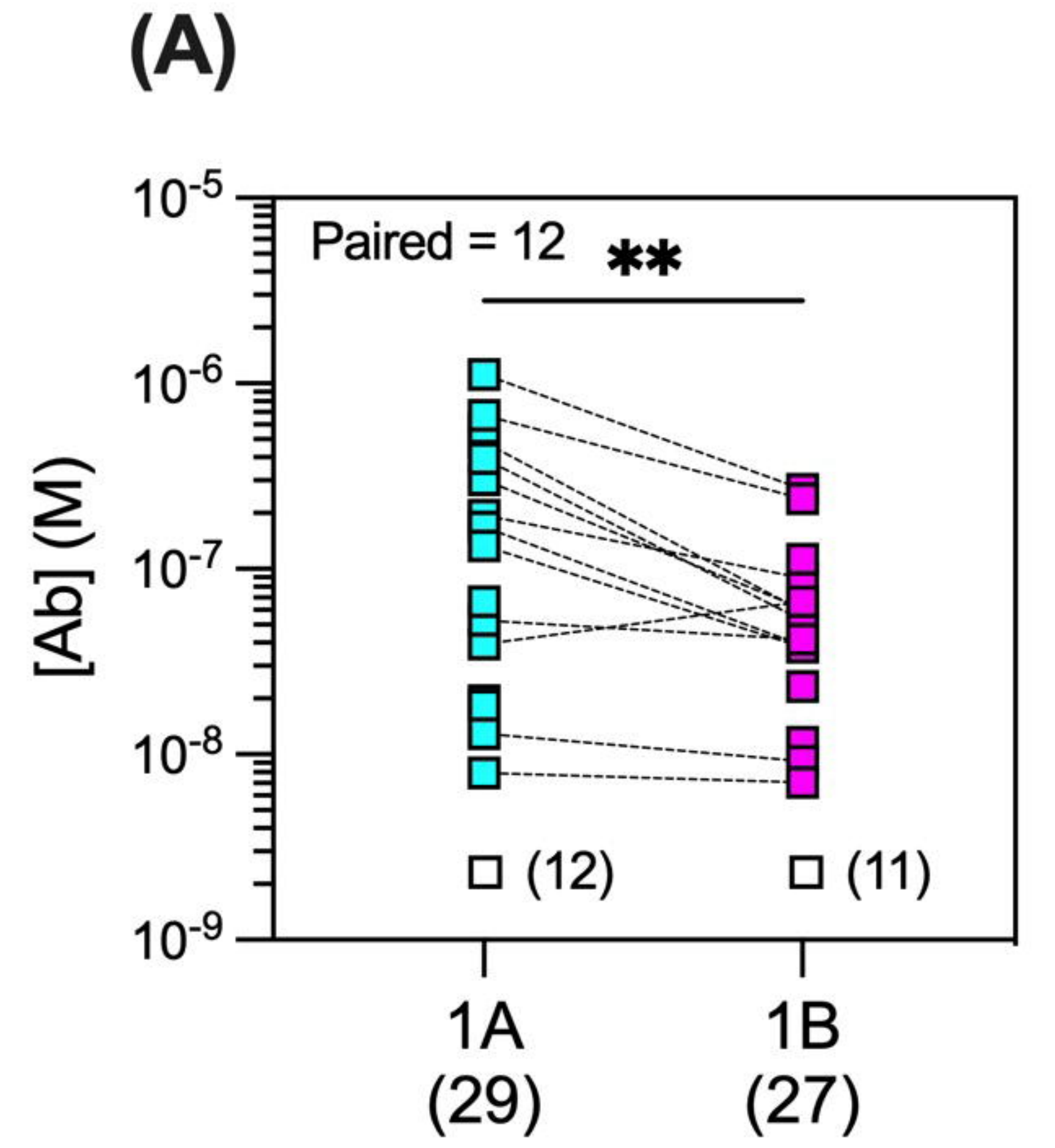
[Ab] (M)

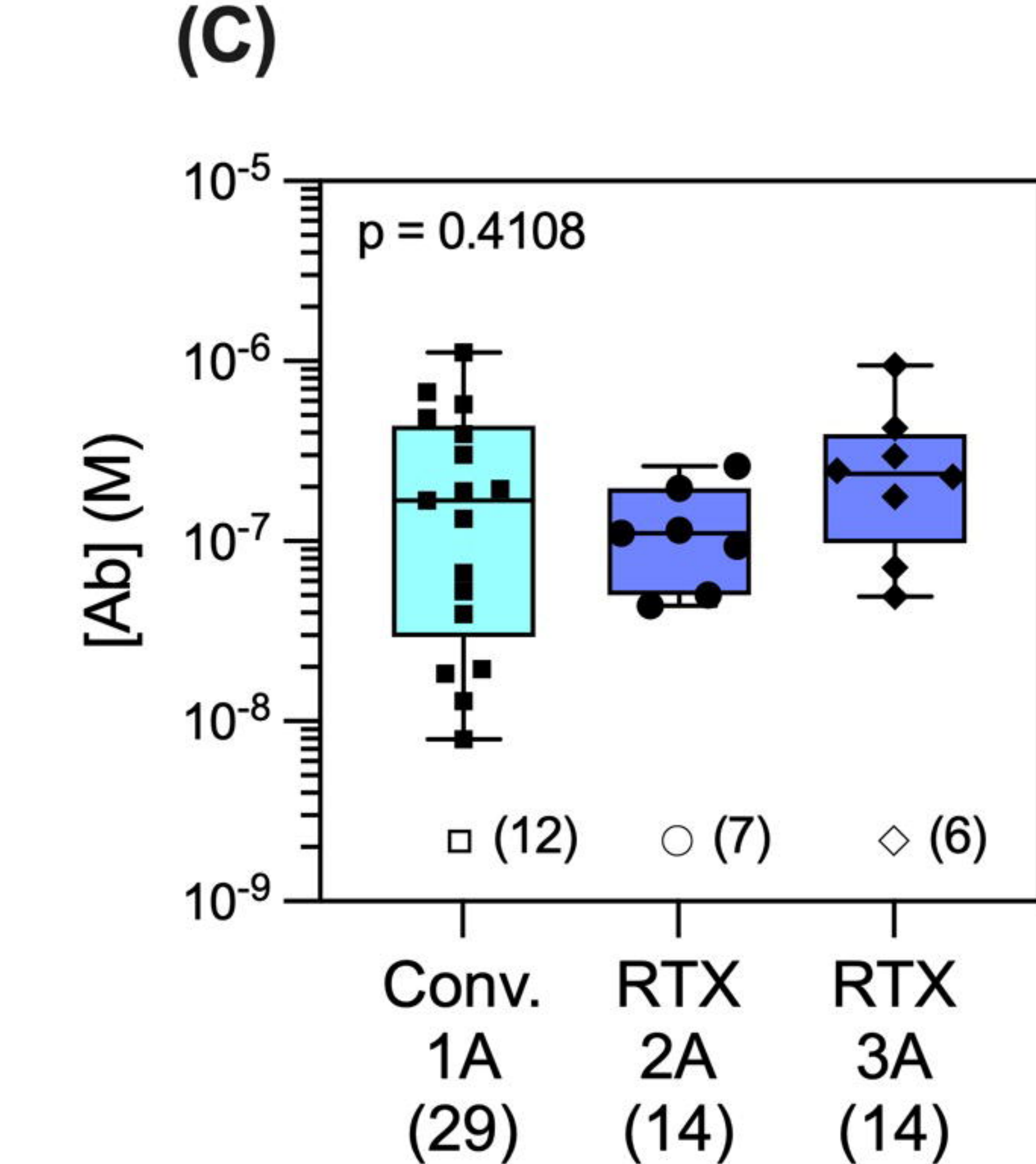
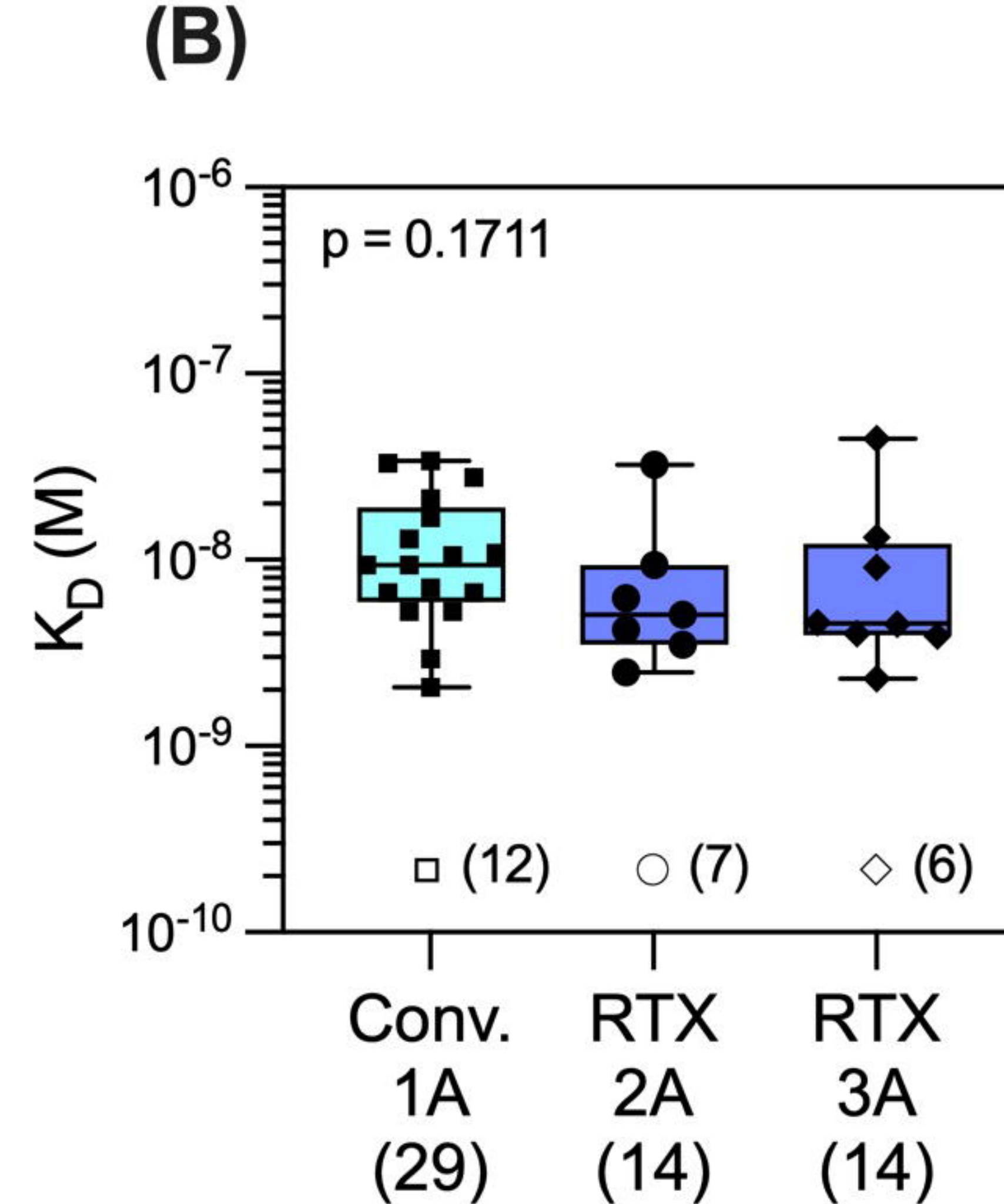
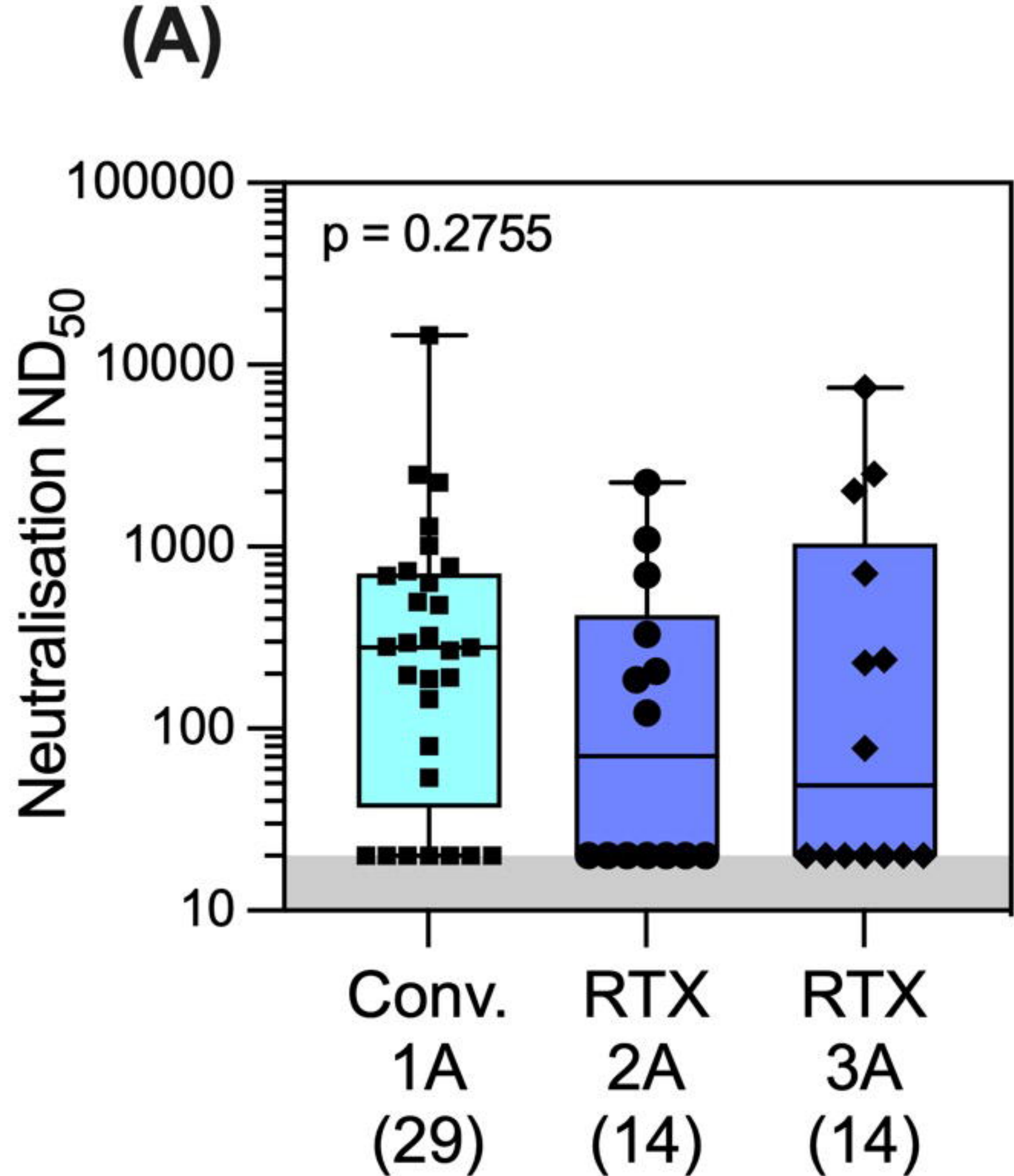


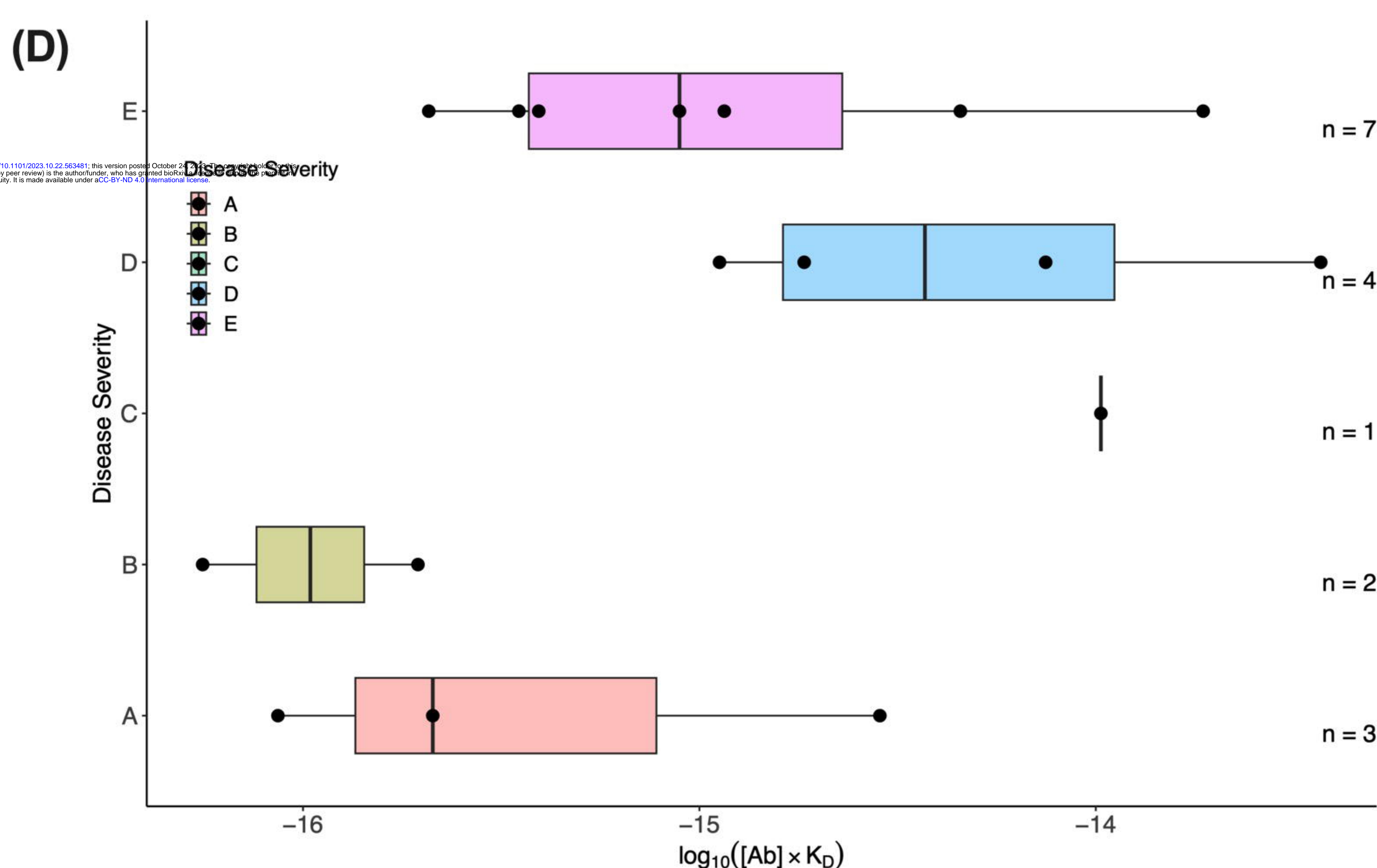
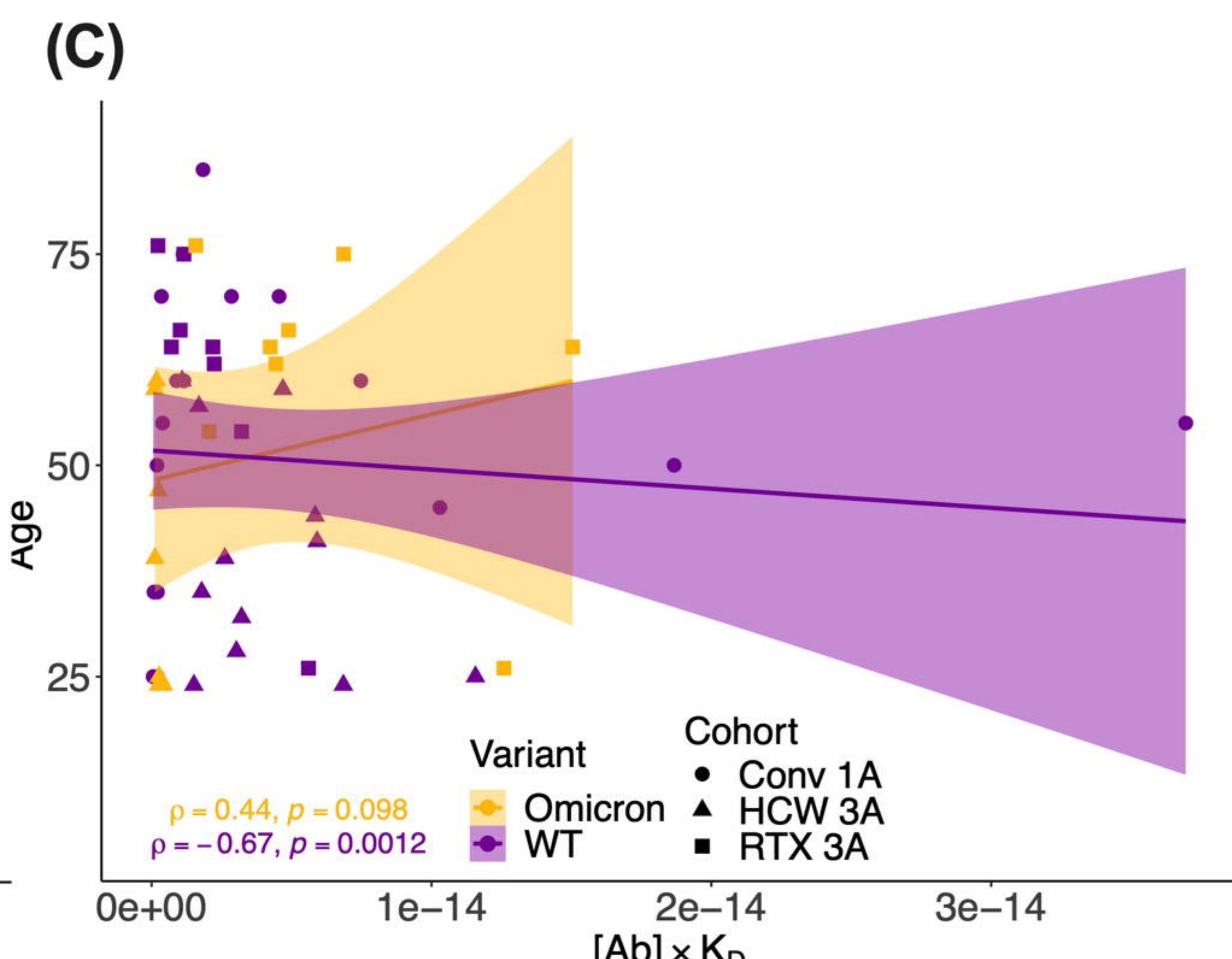
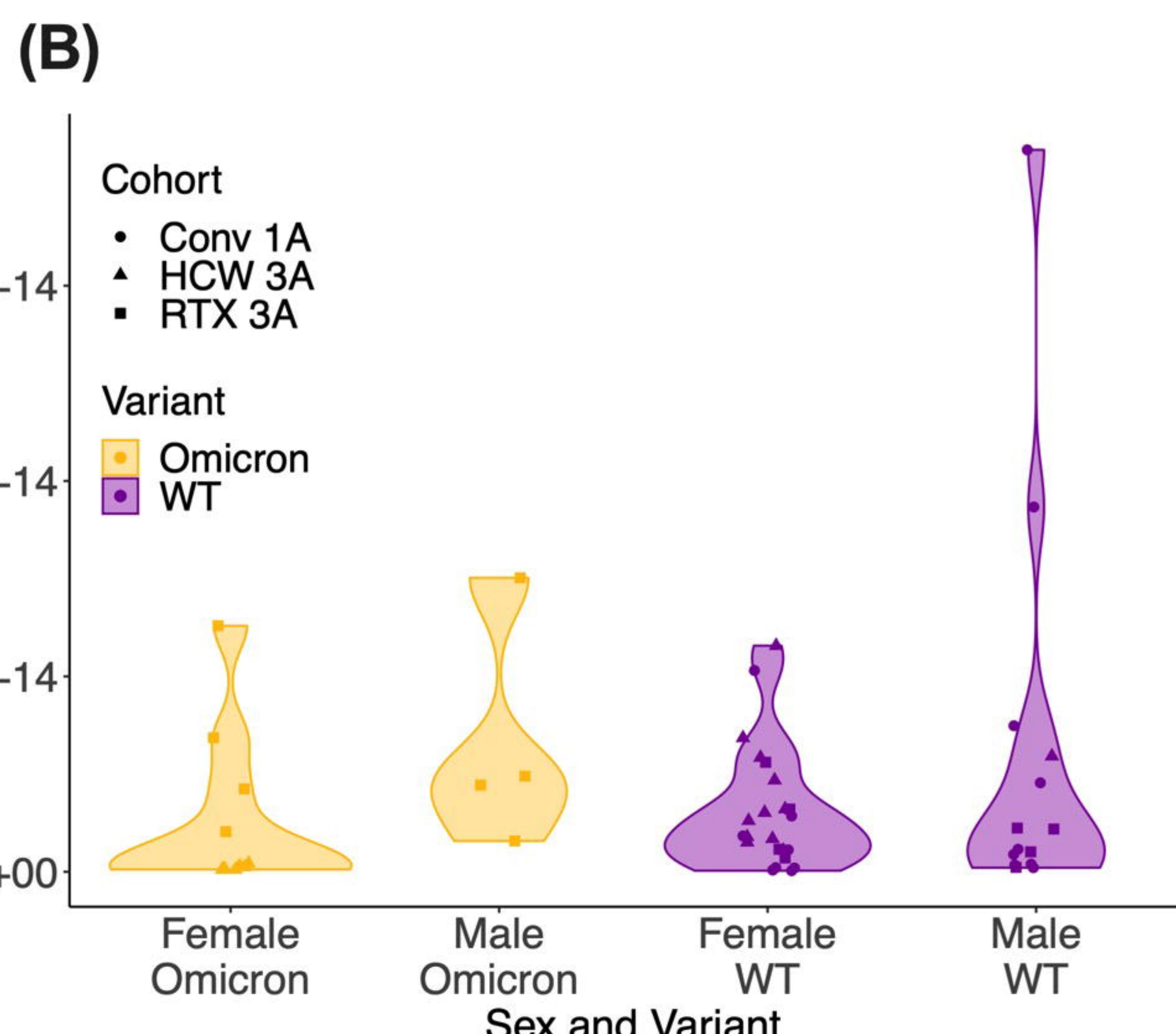
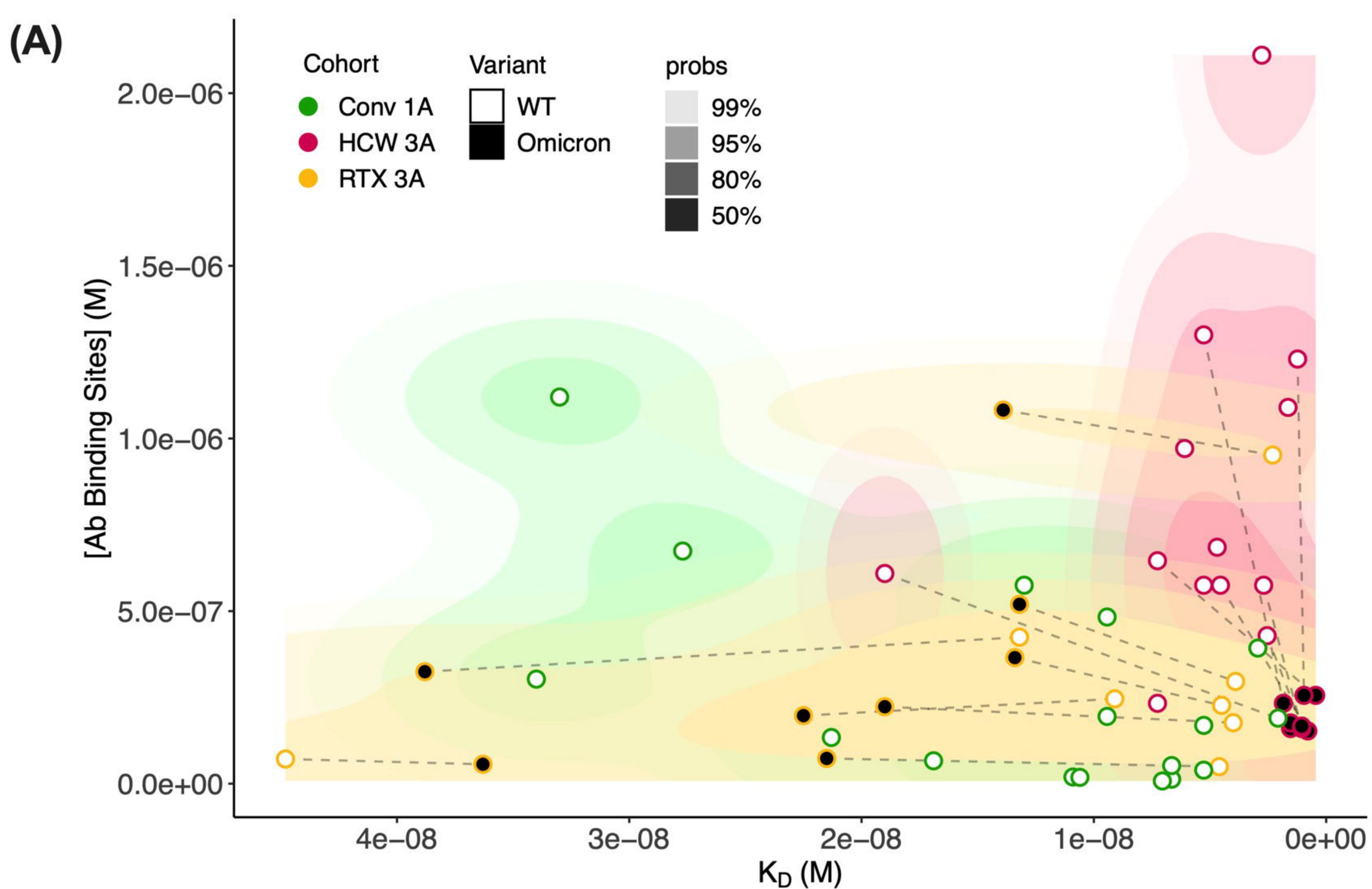
(F)



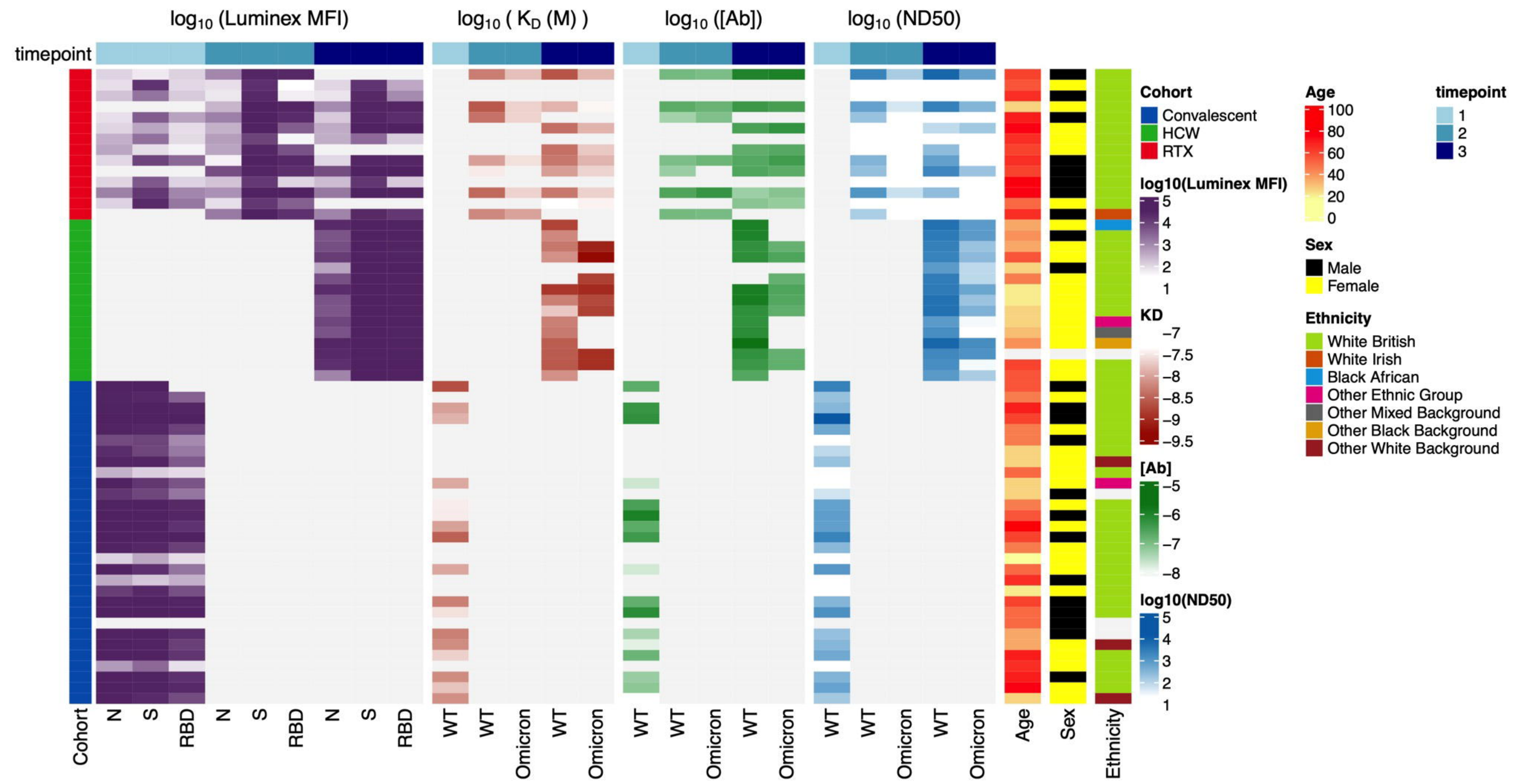
bioRxiv preprint doi: <https://doi.org/10.1101/2023.10.22.563481>; this version posted October 24, 2023. The copyright holder for this preprint (which was not certified by peer review) is the author/funder, who has granted bioRxiv a license to display the preprint in perpetuity. It is made available under aCC-BY-ND 4.0 International license.



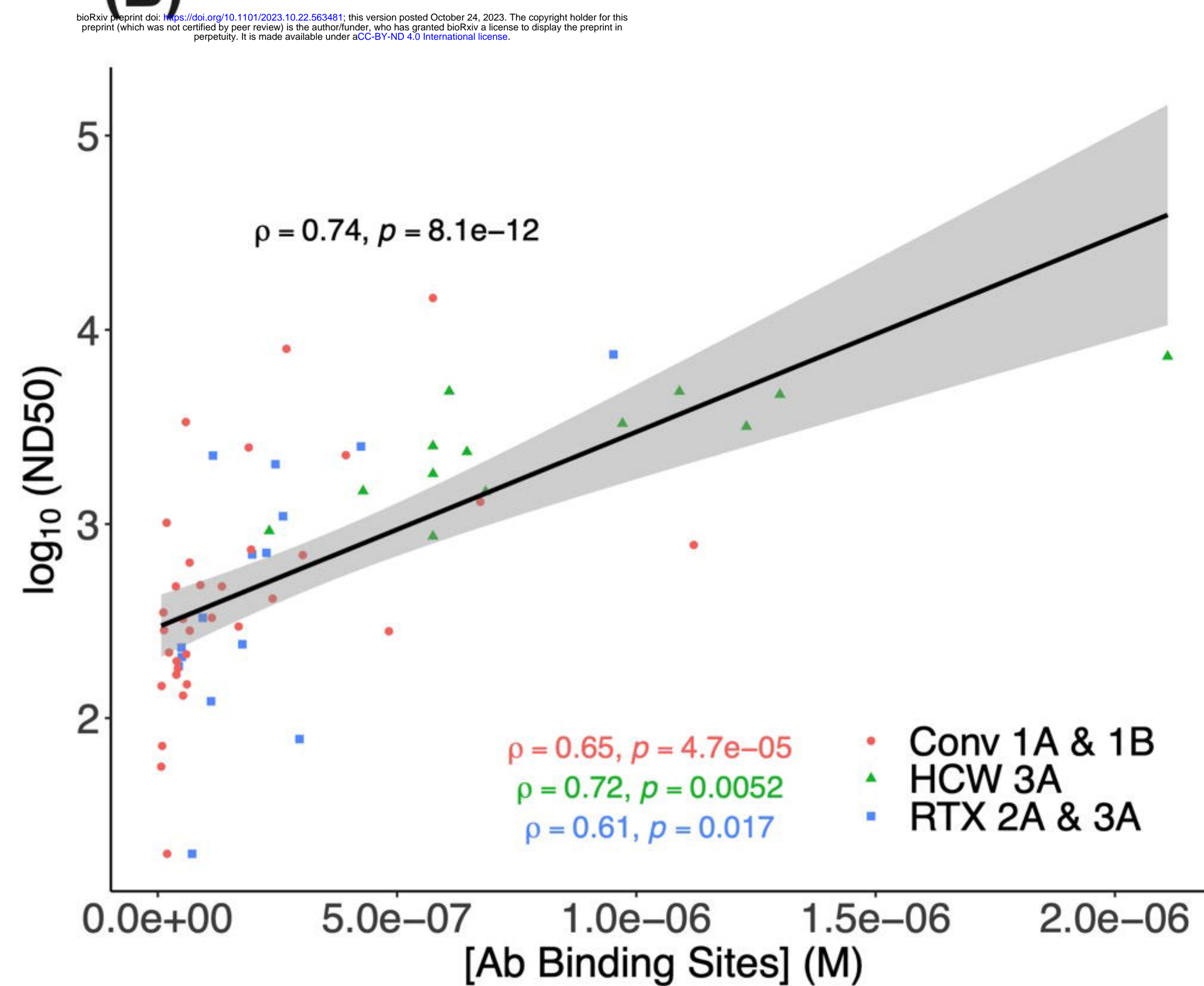




(A)



(B)



(C)

